Dispersion-related description of temperature dependencies of band gaps in semiconductors

Roland Pässler*
Technische Universität Chemnitz, Institut für Physik, D-09107 Chemnitz, Germany
(Received 13 February 2002; revised manuscript received 21 May 2002; published 5 August 2002)

We have developed a novel dispersion-related model for monotonic temperature dependencies of fundamental band gaps, $E_g(T)$, and the associated excitonic absorption and emission line positions, $E_{gx}(T)$, which is suitable for detailed numerical analyses of experimental data available for a large variety of semiconductor (including wide-band-gap) materials and quantum-well structures. The present model is distinguished from preceding ones by the following features: (i) It is applicable to an unusually large span of magnitudes for the phonon dispersion coefficient, $\Delta \equiv \sqrt{\langle(\hbar\omega-\hbar\overline{\omega})^2\rangle}/\hbar\overline{\omega}$, extending from the familiar Bose–Einstein regime of *vanishing* dispersion, $\Delta \geqslant 0$, up to the limiting regime of *extremely large* dispersion, $\Delta \leqslant 1$. (ii) The resulting analytical $E(T)$ functions approach, in the *cryogenic* region, *quadratic* asymptotes, the curvatures of which are throughout significantly *weaker* than suggested by Varshni's *ad hoc* model. (iii) The novel analytical expressions enable direct, straightforward determinations of the $T \to 0$ limits of gap widths, the high-temperature limits of slopes, the average phonon temperatures, $\Theta \equiv \hbar\overline{\omega}/k_B$, and the associated dispersion coefficients, Δ, *without* requiring preliminary determinations of other (auxiliary) quantities. Results of least-mean-square fittings for a variety of group IV, III–V, and II–VI materials are given and compared with those obtained in previous studies using less elaborate models. The parameter sets obtained suggest that the physically realistic range of dispersion coefficients is confined to an interval from 0 up to a *maximum* of about 3/4. Another, qualitatively different, dispersion-related model, which represents the hypothetical regime of extremely large dispersion, $\Delta > 1$, is also developed in this paper solely for the sake of a detailed dispersion-related analysis of Varshni's model function. Our analytical and numerical study concludes that *Varshni's* model is associated with a *hypothetical* case of *extremely large* dispersion characterized by a dispersion coefficient significantly higher than unity, $\Delta_V = (\pi^2/6-1)^{-1/2} = 1.245$. This is in clear contradiction to empirical Δ values that range below unity. The relatively large discrepancy between the upper boundary of about 3/4 for realistic Δ values and the high value of $\Delta_V \cong 5/4$ for Varshni's model is the fundamental reason for the usual inadequacy (large degree of arbitrariness) of parameter values resulting from conventional fittings of $E(T)$ data sets using Varshni's formula.

DOI: 10.1103/PhysRevB.66.085201 PACS number(s): 78.20.−e, 71.20.Nr, 63.20.Kr

I. INTRODUCTION

It is known from a wealth of experimental studies that the widths of fundamental band gaps, $E_g(T)$, for a large variety of semiconductor materials (particularly of group IV, III–V, and II–VI materials, including ternary and quaternary alloys) decrease *monotonically* with increasing lattice temperature. Such a temperature-induced shrinkage of the gap width is seen in experiments by, e.g., a monotonic red shift of exciton absorption and emission peak positions, $E_{gx}(T)$, that are observable in bulk samples as well as in associated heterostructures (superlattices, quantum well structures, quantum dots, etc.). These T-dependencies change from relatively weak (apparently quadratic) ones in the cryogenic region to relatively strong ones (approaching linear asymptotes) at temperatures higher than the effective Debye temperatures,[1] Θ_D. The corresponding red shift is of considerable practical importance particularly with respect to semiconductor devices that are intended to operate within a relatively large temperature interval (extending beyond room temperature). A prerequisite for good design of such systems is the availability of sufficiently comprehensive experimental $E_g(T)$ or $E_{gx}(T)$ data sets. In addition to reliable experimental information, it is computationally convenient and theoretically informative to develop an analytical framework that enables one to perform numerical analyses (least-mean-square fits) of $E(T)$ data sets on a *physically reasonable* basis. The problem of constructing a corresponding analytical framework is obviously not a simple one, because the gap shrinkage effect turns out to be, as a rule, the result of a superposition of contributions made by phonons with largely different energies (beginning from the zero-energy limit for acoustical phonons up to the cut-off energy for optical phonons). A particular aggravation of this theoretical problem is the fact that basic features of phonon dispersion that manifest themselves, e.g., in the positions of prominent phonon energy peaks and the relative weights of their contributions to the observable $E(T)$ dependence, may vary significantly from one material to the other. Thus, the analytical framework must be flexible enough to account for these qualitatively large differences in the features of phonon dispersion (regimes of small, intermediate, or large dispersion) among different materials.

In recent years several *dispersion-related* models that are suitable for fittings of $E_g(T)$ dependencies in various dispersion regimes have been presented. Among the qualitatively different analytical approaches published, the structurally simplest one has the form[2]

$$E(T) \cong E(0) - (\alpha\Theta_p/2)\left[\sqrt[p]{1+(2T/\Theta_p)^p}-1\right]. \qquad (1)$$

In this expression the parameter $\alpha \equiv S(\infty)$ represents the $T \rightarrow \infty$ limit of the slope, $S(T) \equiv -dE(T)/dT$ (=entropy[3,4]), Θ_p is comparable with (roughly equal to) the average phonon temperature,[2,5,6] $\Theta_p \approx \Theta \equiv \langle \hbar\omega \rangle / k_B$, and the fractional exponent p is related to the material-specific degree of phonon dispersion,[6] $\Delta \equiv \sqrt{\langle (\hbar\omega - \langle \hbar\omega \rangle)^2 \rangle} / \langle \hbar\omega \rangle$, by the approximate relation[5] $\Delta \approx 1/\sqrt{p^2-1}$. It has been shown in Ref. 5 for a variety of group IV, III–V, and II–VI materials that this model function (1) (''*p*-representation'') provides best fits of measured $E(T)$ data sets, with standard deviations significantly smaller than those associated with Varshni's *ad hoc* model[3,7] or expressions of Bose–Einstein type.[8–16] Similarly successful have also been applications of Eq. (1) to numerical fittings of temperature dependencies of exciton line positions measured in ternary compounds[17,18] and quantum well structures.[19–23]

However, a detailed assessment of the parameter sets associated with a variety of least-mean-square fittings[5,17–23] using Eq. (1) shows that, due to the relative simple analytical structure (the approximate nature) of this model function, the fitted parameter values Θ_p and p often do not yield good values for the two relevant lowest-order moments,[6] $\langle \hbar\omega \rangle \equiv k_B\Theta$ and $\langle (\hbar\omega)^2 \rangle \equiv (1+\Delta^2)(k_B\Theta)^2$. Particularly in the regime of *small* dispersion,[5,18,20,22] $p > 3$, the model-specific temperature parameter Θ_p tends to be about 20% *lower* than the actual magnitude of the effective (average) phonon temperature Θ (cf. Sec. 3 of Ref. 5). It is true that a moderate underestimate of Θ values like that from Eq. (1) may not have severe consequences for experiments (numerical simulations, including inter- and/or extrapolations[17,18] of restricted data sets into adjacent temperature regions), because the $E(T)$ curves calculated using Eq. (1) are almost indistinguishable from those resulting from more elaborate dispersion-related models. [Note that possible deviations of comparable theoretical $E(T)$ values resulting from different dispersion-related models are usually limited to an order of only ± 0.2 meV; cf. Ref. 20 and see below.] However, such deviations of Θ_p from true $\Theta \equiv \langle \hbar\omega \rangle / k_B$ values are troublesome when estimating[6] relative weights of the contributions of different parts of the phonon spectrum (e.g., of prominent acoustical and/or optical phonon peaks) to the measured $E(T)$ dependence. This is particularly true for estimations of the dependence $\Theta(x)$ of the effective (average) phonon temperature on the composition ratio, x, for ternary compounds, such as $Zn_{1-x}Mg_xSe$,[17] or $Al_xGa_{1-x}As$,[18] where $\Theta(x)$ can only roughly be estimated from $\Theta_p(x)$ values obtained by fittings using the *p*-representation. This is the motivation behind devising models more elaborate than Eq. (1).

An important partial solution of this problem was given by a relatively easily solvable hybrid model,[6,20] which is based on choosing a normalized weighting function in the form of a linear combination of a *constant* component for *low*-energy (acoustical) phonons with a *singular* component for *high*-energy (optical and short-wavelength longitudinal acoustical) phonons.[6] Numerical fittings using the corresponding analytical $E(T)$ function[6,20] (''ρ-representation'') provided self-consistent values for Θ and Δ. Unfortunately, the applicability of the ρ-representation[6,20] is *a priori* confined to cases of moderate (small and intermediate) dispersion, $0 \leqslant \Delta \leqslant 1/\sqrt{3} = 0.577$. This limitation precludes application of this model to certain materials (particularly to AlSb and CdTe[5,24]) in the regime of large dispersion, $\Delta > 1/\sqrt{3}$.

It is the aim of the present article to develop a more comprehensive and flexible dispersion-related model which is distinguished from preceding ones by the following features:

(1) The new model should apply to all physically relevant regimes of dispersion comprising the whole interval from the Bose–Einstein limit ($\Delta \rightarrow 0$) up to sufficiently *large* magnitudes of the dispersion coefficient (i.e., the experimentally relevant range[24] of $0 \leqslant \Delta \lesssim 3/4$, at least).
(2) The theoretical $E(T)$ function should tend in the cryogenic region to a *quadratic* asymptote, i.e., $[E(0) - E(T)] \propto T^2$ for $T \ll \Theta_D$, in accordance with basic theoretical expectations[7,25–27] as well as experimental observations.
(3) The new model should be suited for the construction of a practicable *analytical* expression that is capable of providing *accurate* (self-consistent) values for the dispersion-related parameters Θ and Δ.
(4) An important additional aim of the model is to be able to represent the final $E(T)$ expression *explicitly* in terms of the *model-independent* parameters Θ and Δ, instead of requiring preliminary determinations of various model-specific auxiliary quantities.[6,24]

The basis for the general semi-empirical theory[2,6] for monotonic $E(T)$ dependencies is sketched briefly in Sec. II. We develop in Sec. III a general $E(T)$ model which enables, above all, the derivation of analytical four-parameter expressions. We show that the total range of applicability of the interpolation formula derived in Sec. III B extends from the Bose–Einstein limit up to moderately large dispersion, $0 \leqslant \Delta \lesssim 3/4$, which is sufficient for practical purposes. Using this novel four-parameter expression we determine in Sec. IV the basic parameter sets for a variety of materials.

In addition we perform in Sec. V a more detailed dispersion-related analysis of Varshni's model function.[3,7] We show that this conventional model is connected with an excessively large degree of phonon dispersion, $\Delta_V \cong 5/4$, which is outside the experimentally relevant range, $0 \leqslant \Delta \lesssim 3/4$. Thus we conclude that Varshni's model is generally incapable of providing physically adequate interpretations of available $E(T)$ data sets.

II. SEMI-EMPIRICAL DESCRIPTION OF MONOTONIC $E(T)$ DEPENDENCIES

To understand our subsequent analytical expansions it is sufficient to sketch briefly the analytical basis of the corresponding semi-empirical theory[2,6] for monotonic $E(T)$ dependencies. This dispersion-related theory is in accordance with the generally accepted observation that the gap shrinkage effect in semiconductors is the result of the *cumulative* effect of electron-phonon interaction (EPI) and thermal lattice expansion (TLE). It is based further on the observation[6] that *both* types of contributions to the observable $E(T)$ dependence, that are made by the individual phonon modes $j\mathbf{q}$

(j=branch and $\mathbf{q}$=wave vector, with phonon energies $\varepsilon_{j\mathbf{q}} \equiv \hbar\omega_{j\mathbf{q}}$), are known to vary with lattice temperature just as the Bose–Einstein occupation factors, $\overline{n}(\varepsilon_{j\mathbf{q}},T) = [\exp(\varepsilon_{j\mathbf{q}}/k_BT)-1]^{-1}$ (for more details see Ref. 6 and papers quoted therein). Taking together all contributions made by phonon modes $j\mathbf{q}$ with the same energy, $\varepsilon_{j\mathbf{q}}=\varepsilon$, we could thus represent the resulting $E(T)$ dependence by a unique integral of the form[6]

$$E(T)=E(0)-\int d\varepsilon f(\varepsilon)\cdot\overline{n}(\varepsilon,T), \tag{2}$$

where the relevant spectral function is given by the sum, $f(\varepsilon)=f^{\mathrm{EPI}}(\varepsilon)+f^{\mathrm{TLE}}(\varepsilon)$, of qualitatively different components due to both mechanisms, and $\overline{n}(\varepsilon,T)=[\exp(\varepsilon/k_BT)-1]^{-1}$ represents the thermally averaged phonon occupation number in the corresponding spectral region. Expanding the latter for high temperatures, $T\gtrsim\Theta_D$, in the form of a Taylor series, $\overline{n}(\varepsilon,T)\rightarrow k_BT/\varepsilon-1/2+\varepsilon/(12k_BT)-\ldots$, we see readily that the high-temperature limiting magnitude of the slope of the $E(T)$ dependence (2) is given by the integral

$$\alpha\equiv-\left.\frac{dE(T)}{dT}\right|_{T\rightarrow\infty}=k_B\cdot\int d\varepsilon\,\frac{f(\varepsilon)}{\varepsilon}. \tag{3}$$

For a variety of semiconductors and insulators, particularly of group IV, III–V, and most II–VI materials (including their ternary and quaternary alloys as well as various other binary or ternary compounds), the spectral function $f(\varepsilon)$ in Eqs. (2) and (3) can be inferred from measured $E(T)$ dependencies to be essentially a *positive semi-definite* function of ε throughout the *whole* spectrum of phonon energies, $f(\varepsilon)\geqslant 0$. [Note that there are exceptions, e.g., ternary compounds $Hg_{1-x}Cd_xTe$, $0.17<x<0.5$,[28] where $f(\varepsilon)$ is obviously negative; or CuCl,[29] where $f(\varepsilon)$ changes its sign between the sections of acoustical and optical phonons.] Consequently, with respect to the numerous cases of semi-definite $f(\varepsilon)$ functions, it is convenient to introduce a *normalized, positive semi-definite weighting* function defined by

$$w(\varepsilon)\equiv\frac{k_Bf(\varepsilon)}{\alpha\varepsilon}, \tag{4}$$

[so that $\int d\varepsilon w(\varepsilon)=1$, in accordance with Eq. (3)]. In terms of Eq. (4) we can thus rewrite the integral (2) in the equivalent form

$$E(T)=E(0)-\frac{\alpha}{k_B}\int d\varepsilon\,\frac{w(\varepsilon)\varepsilon}{\exp(\varepsilon/k_BT)-1}. \tag{5}$$

It is instructive to briefly consider some general features of the corresponding monotonic $E(T)$ dependencies (5) for ranges of relatively low (cryogenic) and high temperatures.

A. Low-temperature behavior

Let us consider the weighting function (4) with respect to a certain *low*-energy region, i.e., for $0\leqslant\varepsilon\ll k_B\Theta_D$ at least (corresponding to the edge region of *long*-wavelength acoustical phonons), to be representable by a Taylor series,

$$w(\varepsilon)=\sum_{n=0}^{(\infty)}\frac{w^{(n)}(0)}{n!}\varepsilon^n \tag{6}$$

[where the coefficients $w^{(n)}(0)$ represent the nth order derivatives of $w(\varepsilon)$ at $\varepsilon=0$]. Inserting Eq. (6) into Eq. (5), going to a dimensionless integration variable $z\equiv\varepsilon/k_BT$, and observing that, for $T\ll\Theta_D$, the integrals for the individual ε^n terms can be well approximated by

$$\int_0^\infty dz\,\frac{z^{n+1}}{e^z-1}=(n+1)!\,\zeta(n+2), \tag{7}$$

[where the low order values of Riemann's ζ-functions are $\zeta(2)=\pi^2/6=1.645$, $\zeta(3)=1.202$, $\zeta(4)=\pi^4/90=1.082$,...], we come to a series expansion of the form

$$E(T)\rightarrow E(0)-\frac{\alpha}{k_B}\sum_{n=0}^{(\infty)}(n+1)\zeta(n+2)w^{(n)}(0)(k_BT)^{n+2}. \tag{8}$$

This means that the $E(T)$ dependence in the $T\rightarrow 0$ limit is dominated by a *quadratic* asymptote, $E(T)\rightarrow E(0)-w(0)\times(\pi^2/6)\alpha k_BT^2$, provided that the weighting function (4) is *nonvanishing* in the $\varepsilon\rightarrow 0$ limit, $w(0)>0$.

The occurrence of a quadratic low temperature asymptote had already been predicted many years ago in several theoretical studies.[25–27] Unfortunately, this was misrepresented later in Varshni's *ad hoc* formula[3,7] (for more details see Secs. IV and V). Nevertheless, the expectation of an essentially quadratic low-temperature asymptote seems to be in accordance with experimental observations for a large variety of materials (cf. in particular Ref. 6 and see below). Thus we have a good chance of coming to an adequate analytical model for $E(T)$ dependencies if we chose for the $w(\varepsilon)$ dependence in Eq. (5) a model function which, apart from various other details (cf. Sec. III and Appendices A and B), is generally *nonvanishing* in the *zero* phonon energy limit, $w(0)>0$.

B. Intermediate- to high-temperature behavior

Consider now the argument $x\equiv\varepsilon/k_BT$ of the exponential function [in the denominator of the integral (5)] for the whole spectrum of phonon energies, $0\leqslant\varepsilon\lesssim k_B\Theta_D$, to be smaller than 2π. Accordingly we can represent the corresponding terms of the integrand in Eq. (5) by a Taylor expansion of type $x/(e^x-1)=1-x/2+x^2/12-x^4/720+\ldots$. The $E(T)$ dependence (5) reduces thus, for $T>\Theta_D/2$, to a series expansion of the universal form[6]

$$E(T)=E(0)-\frac{\alpha}{k_B}\cdot\left(k_BT-\frac{\langle\varepsilon\rangle}{2}+\frac{\langle\varepsilon^2\rangle}{12k_BT}-\frac{\langle\varepsilon^4\rangle}{720(k_BT)^3}+\frac{\langle\varepsilon^6\rangle}{30\,240(k_BT)^5}-\ldots\right), \tag{9}$$

where we have denoted by

$$\langle\varepsilon^m\rangle\equiv\int d\varepsilon\,\varepsilon^m\cdot w(\varepsilon),\quad\text{for}\quad m=1,2,4,6,..., \tag{10}$$

the associated moments of the total phonon energy spectrum. The position of the center of gravity ($m=1$) with respect to the temperature scale is represented in analytical $E(T)$ models by an effective (average) phonon temperature,

$$\Theta \equiv \langle \varepsilon \rangle / k_B . \tag{11}$$

The occurrence of phonon dispersion, which is expressed by the difference between the second moment and the square of the first moment, can be conveniently quantified by the dispersion coefficient[6]

$$\Delta \equiv \sqrt{\langle \varepsilon^2 \rangle - \langle \varepsilon \rangle^2} / \langle \varepsilon \rangle . \tag{12}$$

In terms of these basic, dispersion-related parameters Θ (11) and Δ (12) we can rewrite the low order part (up to the $1/T$ term) of the series expansion (9) in the equivalent form

$$E(T) \rightarrow E(0) - \alpha \left(T - \frac{\Theta}{2} + \frac{(1+\Delta^2)\Theta^2}{12T} \right). \tag{13}$$

III. REPRESENTATIVE ANALYTICAL MODEL

For a perfect (nonapproximate) numerical description of the $E(T)$ dependence it would be necessary to know in detail the weighting function, $w(\varepsilon)$, throughout the whole phonon spectrum of a given material. Such detailed microscopic information is usually not available. Moreover it is obvious that, except for the idealized model representation[6,24] of $w(\varepsilon)$ by discrete (δ-functionlike) peaks, exact calculations of integrals of type (5) are, as a rule, very cumbersome and time-consuming for any more realistic form of the weighting function. In view of the unsuitability of such a rigorous procedure, for many practical purposes it is thus useful and sufficient to approximate $w(\varepsilon)$ by a somewhat simpler, analytical model function.

A convenient model for a normalized weighting function, $w(\varepsilon)$, which will be seen below to reasonably satisfy the series of requirements quoted in Sec. I, is given by a class of functions of type $w_\sigma(\varepsilon) \propto (1-\varepsilon/\varepsilon_o)^{\sigma-1}$ (A1), where $\sigma>0$ [for ε up to a certain cut-off energy, $0 \leqslant \varepsilon \leqslant \varepsilon_o$, and $w_\sigma(\varepsilon) = 0$ elsewhere; see Fig. 1 and Appendix A]. For a parameter range of $0<\sigma<1$ the model functions $w_\sigma(\varepsilon)$ (A1) are monotonously *in*creasing, with increasing ε (cf. Fig. 1). The associated dispersion coefficients follow from Eq. (A4) to lie within the range $0<\Delta<3^{-1/2}$, which corresponds to the regime of *moderate* (small to intermediate) dispersion.[6] On the other hand, for a parameter range of $1<\sigma<+\infty$, the model functions $w_\sigma(\varepsilon)$ (A1) are monotonously *de*creasing, with increasing ε (cf. Fig. 1). From Eq. (A4) it follows that the corresponding dispersion coefficients lie within a range of $3^{-1/2}<\Delta<1$. The class of model functions (A1) thus also comprises a relatively broad section of the regime of *large* dispersion. [Note that the total interval of Δ values comprised by the present model, $0 \leqslant \Delta < 1$, is thus even more extensive than the experimentally relevant interval of about $0 \leqslant \Delta \leqslant 3/4$; cf. point (1) in Sec. I.]

Inserting the model function $w_\sigma(\varepsilon)$ (A1) into Eq. (5) and including Eq. (A5) we can write the $E(T)$ dependence (5) in a general form

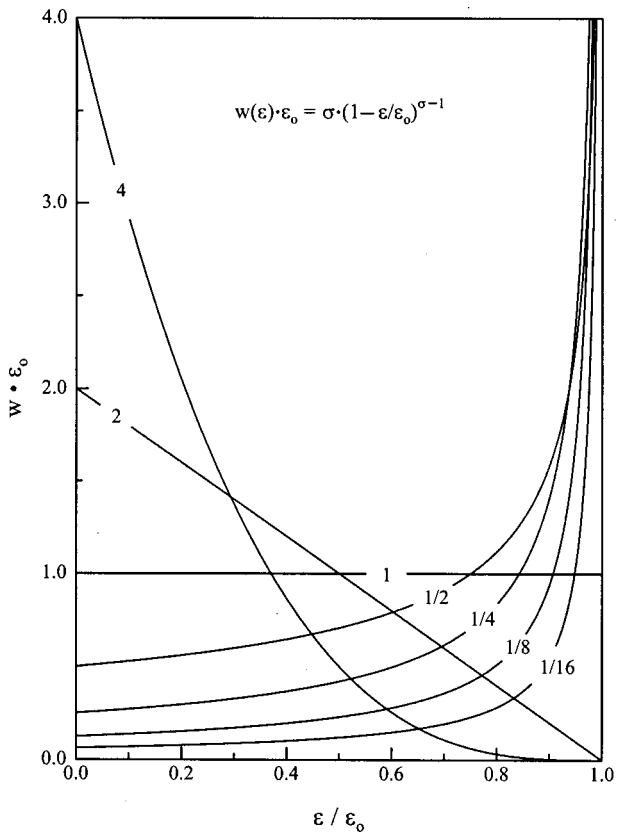

FIG. 1. ε-dependencies of monotonically *increasing* or *decreasing* weighting functions of type (A1), for various discrete parameter values $\sigma<1$ and $\sigma>1$, for *moderate* (small to intermediate), and *large* dispersion, respectively.

$$E(T) = E(0) - \frac{\alpha\Theta}{2}\,\eta\left(\frac{2T}{\Theta}\right), \tag{14}$$

where the characteristic (dimensionless) shape functions η are defined, in terms of the dimensionless ratio $\xi \equiv 2T/\Theta$ and the parameter $\sigma>0$, by integrals of the form (A6). The behaviors of these shape functions $\eta_\sigma(\xi)$ in the limiting regions of low and high temperatures [corresponding to ξ-regions of $\xi<(\sigma+1)/10$ and $\xi>(\sigma+1)\pi$] are given by the analytical expressions (A7) and (A8), respectively.

A. Analytical approximation for moderate and large dispersion ($1/3 \leqslant \Delta < 1$)

Both limiting behaviors represented by Eqs. (A7) and (A8) can be readily seen to be satisfied by an analytical ansatz of the form

$$\eta_\Delta(\xi) = \sqrt[6]{1 + \sum_{n=2}^{4} a_n(\Delta)\xi^n + \xi^6} - 1, \tag{15}$$

where the second and fourth order expansion coefficients are given by

$$a_2(\Delta) = \pi^2\Delta^2/(1+\Delta^2) \quad \text{and} \quad a_4(\Delta) = 2(1+\Delta^2). \tag{16}$$

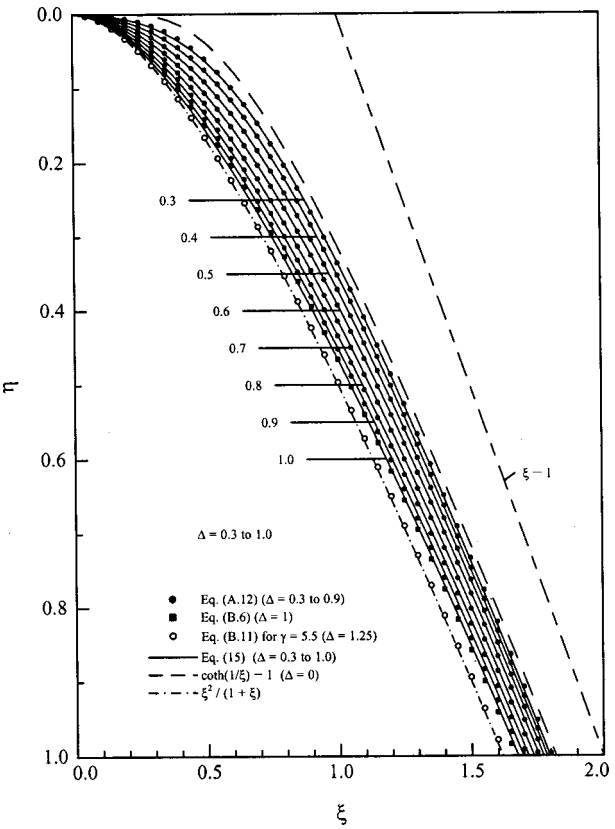

FIG. 2. Characteristic shape functions $\eta_\Delta(\xi)$ for *intermediate* and *large* dispersion, $0.3 \leqslant \Delta \leqslant 1$. The approximate values following from the sixth root representation (15) [with coefficients $a_n(\Delta)$ given by Eqs. (16) and (17)] are nearly equal to exact $\eta_\sigma(\xi)$ values obtained by numerical integration of Eqs. (A12), (A6), or (B6), for $0<\sigma<1$, $1<\sigma<\infty$, and $\sigma\to\infty$, respectively. A numerical comparison of a shape function of Varshni type, $\eta_V(\xi)\equiv\xi^2/(1+\xi)$, with a shape function $\eta_\gamma(\xi)$ (B11) resulting from a weighting function model of type (B7) is also included. The approximate equality of both functions, for a parameter value of $\gamma=5.5$, shows that Varshni's model corresponds to an excessively large (physically unrealistic) Δ of about 1.25 [according to Eq. (B9)].

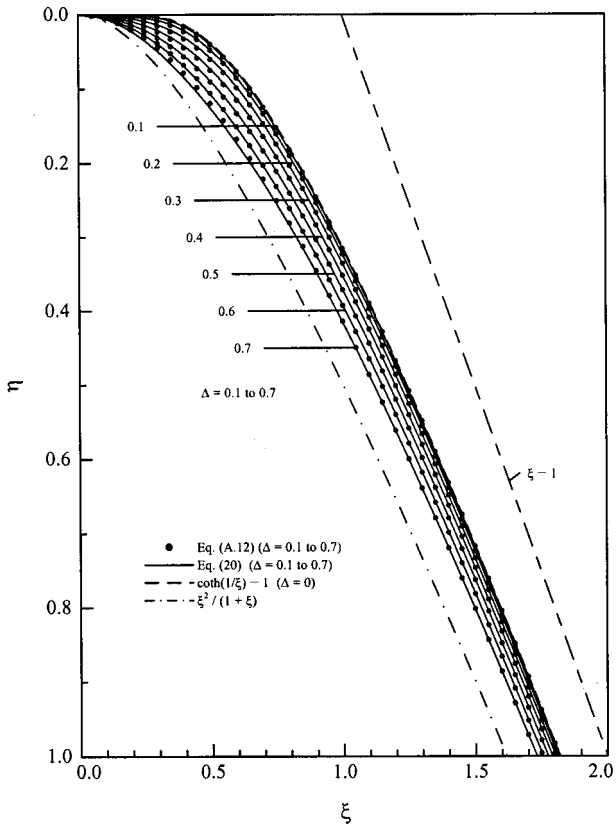

FIG. 3. Characteristic shape functions $\eta_\Delta(\xi)$ for *small, intermediate*, and moderately *large* dispersion, $0 \leqslant \Delta \leqslant 0.7$. The approximate values from the elaborate interpolation formula (20) (with coefficients $c_n(\Delta)$ given by Eqs. (21) and (22)) are nearly equal to exact $\eta_\sigma(\xi)$ values obtained by numerical integration of Eq. (A12) or (A6), for $0<\sigma<1$ and $1<\sigma<2$, respectively.

The remaining third order coefficient $a_3(\Delta)$ affects the behavior of the approximate shape function (15) especially in the range from low to intermediate temperatures (corresponding to ξ-values of the order of unity, Fig. 2). A reasonable analytical approximation for the latter can thus be found by requiring that the analytical formula (15) represents a good approach to the original integral (A6) particularly in this region of intermediate ξ values. By comparing results obtained via numerical integration [using Eq. (A6), for $1<\sigma$, or (A12), for $0<\sigma<1$] with approximate results from Eq. (15) we have found that adequate approximations for $a_3(\Delta)$ are given by

$$a_3(\Delta)\cong 1-4\Delta^2+3\Delta^4, \quad \text{for} \quad 1/3<\Delta\leqslant 1/\sqrt{2} \qquad (17a)$$

and

$$a_3(\Delta)\cong(1-3\Delta^2)/2, \quad \text{for} \quad 1/\sqrt{2}\leqslant\Delta<1. \qquad (17b)$$

This coefficient reduces thus to zero, $a_3(\Delta_c)\to 0$, just at the point of transition, $\Delta\to\Delta_c=3^{-1/2}$, between the regimes of intermediate and large dispersion. Note that both approximate expressions, (17a) and (17b), for the third order coefficient give the same value, $a_3(2^{-1/2})=-1/4$, for $\Delta=2^{-1/2}=0.707$, and that its magnitudes are *small* throughout in comparison with those of the fourth order coefficient (16), $2\leqslant a_4(\Delta)\leqslant 4$.

We have plotted in Fig. 2 a series of $\eta_\Delta(\xi)$ curves following from Eq. (15), with Δ-dependent expansion coefficients given by Eqs. (16) and (17a/b), for equidistant Δ values pertaining to the regimes of intermediate and large dispersion. The bold circles in Fig. 2 represent the exact values obtained by numerical integration of the first version of Eq. (A6), for $1\leqslant\sigma$, or Eq. (A12), for $0<\sigma<1$. The comparison of the latter with approximate results (solid curves) in Fig. 2 shows that, due to the specification of expansion coefficients by Eqs. (16) and (17a/b), the sixth root expression (15) is a good approximation to the characteristic shape functions for dispersion coefficients within a range of about $1/3<\Delta<1$, at least.

Replacing, henceforth, the original (exact) shape function $\eta_\sigma(\xi)$ (A6) [=(A12)] in Eq. (14) by $\eta_\Delta(\xi)$ (15) we can describe the $E(T)$ dependencies, for regimes of *intermediate* and *large* dispersion, to a good approximation by an analytical expression of the form

$$E(T)=E(0)-\frac{\alpha\Theta}{2}\times\left(\sqrt[6]{1+\sum_{n=2}^{4}a_n(\Delta)\left(\frac{2T}{\Theta}\right)^n+\left(\frac{2T}{\Theta}\right)^6}-1\right). \quad (18)$$

B. Overall formula for small, intermediate, and larger dispersion ($0\leqslant\Delta\lesssim 3/4$)

Analytical models of Bose–Einstein type[8–16] represent the limiting case of vanishing dispersion, $\Delta\to 0$. The characteristic shape function for this limit, $\eta_B(\xi)\equiv\eta_{\Delta\to 0}(\xi)$, has the form[5]

$$\eta_B(\xi)=\frac{2}{\exp(2/\xi)-1}=\coth\left(\frac{1}{\xi}\right)-1. \quad (19)$$

The latter is obviously not coincident with the $\Delta\to 0$ limit of Eq. (15). This is why a mere root representation like Eq. (15) does not give good results for the regime of small dispersion, $0\leqslant\Delta<1/3$. The latter regime is only rarely seen[5,24] in bulk samples of elemental and binary materials; however it has been found recently in certain ternary compounds[18] and heterostructures.[20,22] Thus, it is desirable for practical applications to find a more general analytical $E(T)$ representation that will give good results within the entire interval of dispersion coefficients Δ relevant to experiments (i.e., from 0 up to about 3/4, at least).

Such an analytical approximation can be constructed via the alternative ansatz

$$\eta_\Delta(\xi)=\frac{2(1-3\Delta^2)}{\exp(2/\xi)-1}+3\Delta^2\left(\sqrt[6]{1+\sum_{n=2}^{4}c_n(\Delta)\xi^n+\xi^6}-1\right), \quad (20)$$

where the Δ-dependent second and fourth order expansion coefficients are given by

$$c_2(\Delta)=\pi^2/(3(1+\Delta^2)) \text{ and } c_4=8/3. \quad (21)$$

We see that in the Bose–Einstein limit, $\Delta\to 0$, the $\eta_\Delta(\xi)$ ansatz (20) coincides with the characteristic Bose–Einstein shape function $\eta_B(\xi)$ (19). Furthermore we find readily, by expanding the expression (20) for the limiting regions $\xi\ll 1$ and $\xi>1$ into a Taylor series, that the corresponding asymptotes actually coincide with Eqs. (A7) and (A8), respectively.

To determine, approximately, the Δ dependence of the coefficient $c_3(\Delta)$ we have done comprehensive numerical comparisons (Fig. 3) between exact $\eta_\sigma(\xi)$ values obtained via numerical integration [in Eqs. (A6) or (A12)] and approximate $\eta_\Delta(\xi)$ values following from Eq. (20). In this way we have found an adequate approximation for $c_3(\Delta)$ to be given by

$$c_3(\Delta)\cong(3\Delta^2-1)/4. \quad (22)$$

The corresponding shape functions (20) are plotted for a series of equidistant values of the dispersion coefficient in Fig. 3. The comparison of these ξ-dependencies (solid curves) with exact values (dots) due to Eq. (A6) or (A12) shows that Eq. (20) represents, in fact, a good analytical approximation within the whole interval $0\leqslant\Delta\leqslant 0.7$ (at least), i.e., from completely vanishing up to moderately large dispersion. Replacing, finally, the original (exact) shape function $\eta_\sigma(\xi)$ (A6) in Eq. (14) by the analytical approximation $\eta_\Delta(\xi)$ (20) we can represent, henceforth, the $E(T)$ dependence explicitly in the form

$$E(T)=E(0)-\alpha\Theta\left\{\frac{(1-3\Delta^2)}{\exp(\Theta/T)-1}+\frac{3\Delta^2}{2}\left(\sqrt[6]{1+\frac{\pi^2}{3(1+\Delta^2)}\left(\frac{2T}{\Theta}\right)^2+\frac{3\Delta^2-1}{4}\left(\frac{2T}{\Theta}\right)^3+\frac{8}{3}\left(\frac{2T}{\Theta}\right)^4+\left(\frac{2T}{\Theta}\right)^6}-1\right)\right\}. \quad (23)$$

Comparing the latter representation with Eq. (18) we see that both analytical approximations are just coincident at the transition point between the regimes of moderate and large dispersion, $\Delta\to\Delta_c=3^{-1/2}$.

IV. SAMPLE RESULTS AND DISCUSSION

On the basis of a physically reasonable model ansatz for the spectral (weighting) function we have derived two elaborate four-parameter expressions for monotonic temperature dependencies of fundamental or excitonic energy gaps, $E_g(T)$ or $E_{gx}(T)$, of semiconductors (including wide-band-gap materials) and associated heterostructures. In contrast to earlier dispersion-related models,[2,6,20,24] applications of which generally involve preliminary estimations of various model-specific auxiliary quantities, the final analytical $E(T)$ expressions derived in the present paper, Eqs. (18) and (23), are given *explicitly* in terms of the dispersion-related parameters Θ (11) and Δ (12) [in combination with α (3) and $E(0)$]. These basic parameters can hence be determined directly via least-mean-square fittings of given $E(T)$ data sets.

The qualitative difference in the analytical structures of the two alternative $E(T)$ expressions derived in Subsections III A and III B is closely related to their specific ranges of

TABLE I. Dispersion-related parameters from numerical fittings of experimental $E_g(T)$ (fundamental band gap) or $E_{gx}(T)$ (exciton peak) data available for various group IV, III–V, and II–VI materials using Eq. (23).

Material	Ref.	$T_{\min} \div T_{\max}$ (K)	$\alpha/10^{-4}$ (eV/K)	Θ (K)	Δ	$\alpha\Theta/2$ (meV)
Diamond	30	103 to 660	(5.0)	(1335)	(0.11)	(334)
SiC (15R)	31	6 to 645	4.67	919	0.32	215
Si	32,33	2 to 415	3.23	446	0.51	72
Ge	34	4 to 416	4.13	253	0.49	52
AlN	35	4 to 298	(9.1)	(770)	(0.34)	(350)
AlAs	36	4 to 287	3.90	256	0.48	50
AlSb	37	4 to 298	3.45	205	0.76	35
GaN	38	2 to 1067	6.14	586	0.40	180
GaP	39,40	4 to 680	4.77	355	0.60	85
GaAs	41,42	2 to 673	4.77	252	0.43	60
GaSb	43,44	9 to 300	3.87	205	0.44	40
InN	45	4 to 300	(2.3)	(590)	(0.35)	(68)
InP	46,47	4 to 873	3.96	274	0.48	54
InAs	48	10 to 300	2.82	147	(0.68)	21
InSb	48,49	10 to 550	2.54	155	(0.36)	20
ZnS	50	2 to 541	5.49	285	0.37	78
ZnSe	50	4 to 500	5.00	218	0.36	55
ZnTe	50	2 to 291	4.68	170	0.37	40
CdS	51/54	2 to 289	4.10	166	0.47	34
CdSe	55	15 to 550	4.08	187	(0.20)	38
CdTe	56	2 to 300	3.08	104	0.69	16

applicability. As we have concluded above from Figs. 2 and 3, Eqs. (18) and (23) represent good (self-consistent) analytical approximations to the original integrals (5) for dispersion coefficients within ranges of about $1/3 \lesssim \Delta < 1$ or $0 \leqslant \Delta \lesssim 3/4$, respectively. Favorable for many practical applications is the relatively large *overlap*, $1/3 \lesssim \Delta \lesssim 3/4$, between the respective ranges of applicability, where *both* formulas give essentially the *same* results (for some typical examples see below). This overlap gives us for many materials, among other things, the opportunity to assess the degree of reliability (unambiguousness) of the outcomes of least-mean-square fitting processes by comparing the results obtained alternatively from Eqs. (18) and (23). Concerning the remaining Δ-regions outside (above or below) this overlap it is important to note that, until now, we could not find any material or heterostructure whose dispersion coefficient appeared to be significantly higher than 3/4. However, there have been found already several materials and heterostructures whose dispersion coefficients are indicative of small dispersion,[18,20,22] $0 \leqslant \Delta < 1/3$ [which is not covered satisfactorily by Eq. (18)]. That is, all Δ values estimated hereto from measured $E(T)$ data sets lie within the range of applicability of Eq. (23), $0 \leqslant \Delta \lesssim 3/4$ (cf. Refs. 2, 6, 20, 24 and see Table I). Consequently, Eq. (23) is of primary importance [superior to Eq. (18)] with respect to numerical analyses of a multitude of monotonic $E(T)$ dependencies associated with qualitatively different dispersion regimes that are actually found in experiment.

In order to compare results of the present model with earlier (approximate or partial) results due to the p-representation,[5] the ρ-representation,[6] and/or the two-oscillator model[24] we performed least-mean-square fittings of the same experimental data sets for group IV,[30–34] III–V,[35–49] and II–VI materials,[50–56] by Eq. (23). The resulting sets of parameters α (3), Θ (11), and Δ (12) are listed in Table I. The associated zero temperature positions, $E_g(0)$ or $E_{gx}(0)$, are not reported because these positions calculated by Eq. (23) are essentially the same (except for tiny numerical differences of order ± 0.1 meV) as those obtained using the earlier (less elaborate) dispersion-related models.[5,6,24] In the last column of Table I we have listed the magnitudes of the corresponding $T=0$ renormalization energies,[57] which are given by the energy separations, $\alpha\Theta/2$, between the fitted $E(0)$ positions and the points of intersection of the linear $T \to \infty$ asymptotes, $E_\infty(T) = E(0) - \alpha(T - \Theta/2)$, with the energy axis, $E_\infty(0) = E(0) + \alpha\Theta/2$, (cf. Fig. 1 in Ref. 6).

According to our semi-empirical description of monotonic $E(T)$ dependencies, there is a *monotonic* relationship (A7) between the relative magnitude of *dispersion*, Δ (12), on the one hand, and the magnitude of the *curvature* of the characteristic low temperature asymptotes, $\eta_\Delta(\xi \ll 1)$ (cf. Figs. 2 and 3), on the other hand. Because to this, the quadratic dependence in the cryogenic region for a given material generally tends to be stronger as the dispersion coefficient gets larger. An instructive example of this is provided by comparing the experimental $E(T)$ data fields for the indirect gap

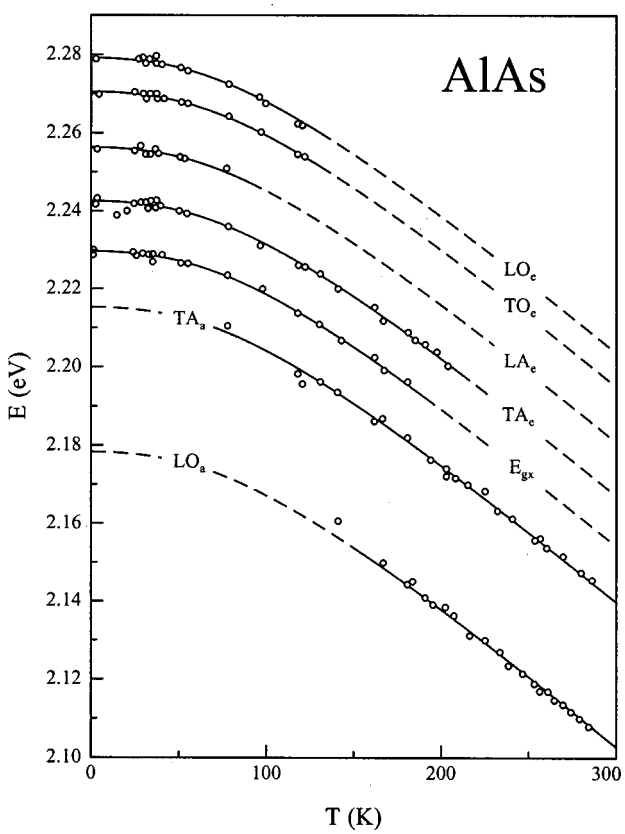

FIG. 4. Temperature dependence of the indirect excitonic band gap, E_{gx}, and of several threshold energies of phonon-assisted transitions observed by Monemar (Ref. 36) near the $\Gamma_{15v}-X_{1c}$ edge of AlAs. The subscripts "*e*" and "*a*" stand for transitions involving an emission or absorption of a LO, TO, LA, or TA phonon. The curves are a comprehensive numerical fit of the *whole* data field using Eq. (23) with a *unique* constellation of basic dispersion-related parameters α, Θ, and Δ (cf. Table I).

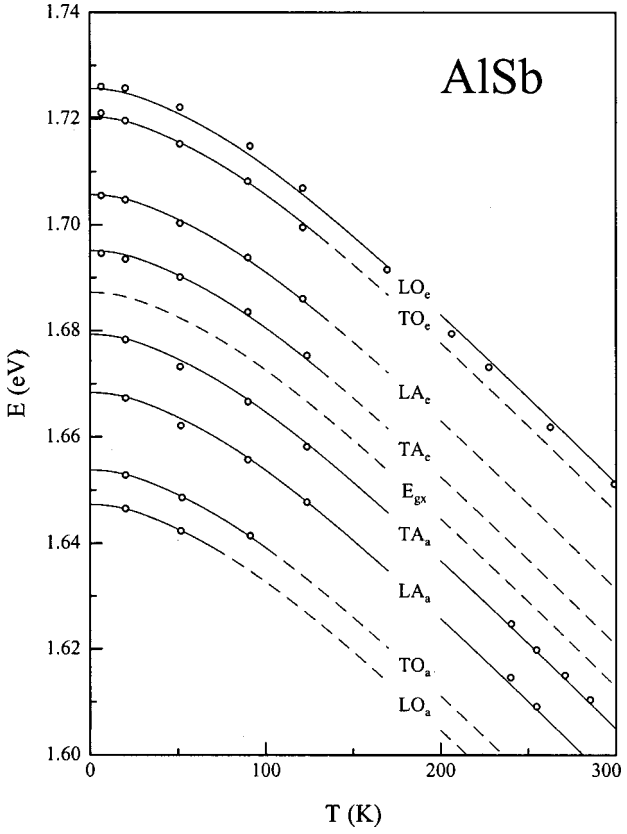

FIG. 5. Temperature dependence of the threshold energies of indirect phonon-assisted transitions observed by Alibert *et al.* (Ref. 37) near the $\Gamma_{15v}-\Delta_{1c}$ edge of AlSb. The subscripts "*e*" and "*a*" stand for transitions involving an emission or absorption of a LO, TO, LA, or TA phonon. The curves are a numerical fit of the *whole* data field using Eq. (23) with a *unique* constellation of basic dispersion-related parameters α, Θ, and Δ (cf. Table I).

III–V materials AlAs[36] and AlSb[37] (see Figs. 4 and 5, respectively). The corresponding temperature dependencies of the indirect excitonic gap in both materials are given in terms of threshold energies of TA, LA, TO, and LO phonon assisted transitions (where the indices "*e*" and "*a*" correspond to processes of phonon emission and absorption, respectively). Taking the corresponding phonon energies to be essentially *constant* within the temperature regions of consideration ($0<T<300$ K) we have performed, consequently, *simultaneous* fittings of the $E(T)$ curves by a *unique* material-specific set of dispersion-related parameters α, Θ, and Δ, in combination with a set of separate zero temperature positions, $E_i(0)$, for the individual phonon assisted transitions.

In the case of AlAs (Fig. 4) we have obtained from fittings by Eq. (23) the parameter values $\alpha=3.90\times10^{-4}$ eV/K, $\Theta=256$ K, and $\Delta=0.48$ (Table I) in combination with $E_{\mathrm{LOe}}(0)=2.2792$ eV, $E_{\mathrm{TOe}}(0)=2.2705$ eV, $E_{\mathrm{LAe}}(0)=2.2563$ eV, $E_{\mathrm{TAe}}(0)=2.2426$ eV, and $E_{gx}(0)=2.2297$ eV for the individual phonon emission processes and the excitonic gap (no-phonon transitions). The extrapolated zero temperature positions for phonon-absorption assisted transitions are $E_{\mathrm{TAa}}(0)=2.2153$ eV and $E_{\mathrm{LAa}}(0)=2.1783$ eV. An alternative fit of the whole data field by Eq. (18) gave approximately the same $T\rightarrow0$ positions (higher by about 0.1 meV) in combination with basic parameters of $\alpha=3.91\times10^{-4}$ eV/K, $\Theta=258$ K, and $\Delta=0.50$. The small difference of only 0.3%, 0.8%, and 4% between the magnitudes α, Θ, and Δ, respectively, as resulting from the alternative fits by Eq. (18) vs Eq. (23), represents the internal consistency of the analytical apparatus developed in Sec. III within the regime of intermediate dispersion, $1/3<\Delta<1/\sqrt{3}$.

For AlSb (Fig. 5) we obtained from fittings by Eq. (23) the parameter values $\alpha=3.45\times10^{-4}$ eV/K, $\Theta=205$ K, and $\Delta=0.76$ (Table I) in combination with $E_{\mathrm{LOe}}(0)=1.7256$ eV, $E_{\mathrm{TOe}}(0)=1.7203$ eV, $E_{\mathrm{LAe}}(0)=1.7057$ eV, $E_{\mathrm{TAe}}(0)=1.6951$ eV, $E_{\mathrm{TAa}}(0)=1.6793$ eV, $E_{\mathrm{LAa}}(0)=1.6683$ eV, $E_{\mathrm{TOa}}(0)=1.6538$ eV, $E_{\mathrm{LOa}}(0)=1.6473$ eV for the individual phonon emission and absorption processes. From this set of zero temperature threshold positions there follows a value of $E_{gx}(0)=1.6869$ eV for the excitonic gap (no-phonon transitions). An alternative fit of the whole data field by Eq. (18) gave again nearly the same $T\rightarrow0$ positions (lower by 0.1 meV) in combination with the basic parameter values $\alpha=3.42\times10^{-4}$ eV/K, $\Theta=199$ K, and $\Delta=0.74$. The moderate difference of about 1% to 3% between the magnitudes of α, Θ, and Δ for Eq. (18) vs. Eq. (23) confirms the compatibility of both analytical approximations even for the

case of large dispersion, $\Delta > 1/\sqrt{3}$.

By comparing now, in more detail, the low-temperature sections of the $E(T)$ curves for both materials, we observe a markedly weaker curvature (second derivative) for AlAs (Fig. 4) than for AlSb (Fig. 5). This qualitative difference in curvatures is directly connected with the quantitative difference between the drops of the respective excitonic gaps measured in the cryogenic region. We see, e.g., from Figs 4 and 5 that the drops $E(0)-E(50\,\mathrm{K})$ amount to about 2.4 meV and 4.6 meV, for AlAs and AlSb, respectively. The relatively large difference (by a factor of about 2) can be readily understood to be a consequence of the largely different magnitudes of the dispersion coefficient in both materials. To this end, we consider the analytical form of the low-temperature asymptote which, according to Eq. (23) or (18) [as well as Eq. (14) in combination with Eq. (A7)], reduces to the quadratic dependence

$$E(T) \rightarrow E(0) - cT^2, \quad \text{where} \quad c \equiv -\frac{1}{2}\left.\frac{d^2E(T)}{dT^2}\right|_{T\rightarrow 0} = \frac{\pi^2\Delta^2\alpha}{3(1+\Delta^2)\Theta}. \tag{24}$$

Inserting the α, Θ, and Δ values listed for both materials in Table I we obtain for the curvature coefficient the values $c = 0.95\times10^{-6}$ eV/K^2, for AlAs, and $c = 1.85\times10^{-6}$ eV/K^2, for AlSb. The difference of a factor of about 2 between the curvature coefficients c (24) explains the corresponding difference in $E(T)$ drops measured for these materials in the cryogenic region. At the same time we find that the ratios α/Θ [occurring as proportionality factors in c (24)] are 1.52×10^{-6} eV/K^2 for AlAs and 1.69×10^{-6} eV/K^2 for AlSb, which corresponds to a difference of only about 11% between these materials. This means that it is the difference between the *dispersion* coefficients Δ of about 0.48 for AlAs and 0.76 for AlSb which, by virtue of the dispersion-related factor $\Delta^2/(1+\Delta^2)$ (in Eq. (24)) of about 0.19 for AlAs and 0.37 for AlSb, represents the *main* cause for the relatively large difference between the respective magnitudes of $E(0)-E(50\,\mathrm{K})$ drops. In this connection it is worth noting that, except for AlSb (and possibly still for InAs, where the available $E(T)$ data[48] are too sparse for an unambiguous quantification), the material-specific $E(0)-E(50\,\mathrm{K})$ drops for *all other* III–V materials listed in Table I are *smaller* than 3 meV. We can thus look upon AlSb as an extreme case, where the significantly stronger $E(0)-E(50\,\mathrm{K})$ drop compared to other III–V materials is due to an exceptionally large degree of dispersion, $\Delta\approx3/4$. As we see from Table I, this value represents the maximum among the Δ values obtained for all group IV, III–V, and II–VI materials considered. According to Eq. (A4), a dispersion coefficient of order $\Delta\approx3/4$ is associated with an order of $\sigma\approx5/2$ for the model-specific parameter in Eq. (A1). This corresponds to a strongly *decreasing* weighting function, $w(\varepsilon)\propto(1-\varepsilon/\varepsilon_o)^{3/2}$ (cf. Fig. 1), indicating an unusually strong contribution of *low*-energy (acoustical) phonons to the gap shrinkage effect in AlSb (in accordance with Ref. 24).

We should note that some of the material-specific parameter sets in Table I are still relatively uncertain. These are given in parentheses. This is mainly due to: (1) the relative *sparsity* and/or *in-accuracy* of experimental data points in the *cryogenic* region (e.g., for diamond,[30] AlN,[35] InN,[45] InAs,[48] InSb,[48] and CdSe,[55] which involve uncertainties in the dispersion coefficient Δ of up to 20%) and/or (2) *limitations* of experimental measurements to temperatures considerably *lower* than the corresponding Debye temperature (to $T<300$ K, for AlN[35] and InN,[45] which involve uncertainties up to 20% for the limiting slope α and the effective phonon temperature Θ).

For most materials listed in Table I (except for nitrides), the uncertainties in α and Θ values are generally limited to a few percent. This applies in particular to Ge,[34] GaAs,[41,42] GaSb,[43,44] InP,[46,47] InAs,[48] InSb[48,49] as well as to zinc and cadmium chalcogenides,[50–56] where the experimental measurements managed to be extended *beyond* the Debye temperatures. Fitting the data sets for the latter cases by using Eq. (18) gave α and Θ values different from those in Table I [of Eq. (23)] by less than 0.5% and 1.5%, respectively.

It is necessary that measurements be made up to the vicinity of the effective Debye temperatures, i.e., $T_{\max}\gtrsim\Theta_D$,[50,58] to enable a reliable determination of α and Θ governing the high-temperature behavior, Eq. (13). This can be well illustrated by the different $E_g(T)$ and $E_{gx}(T)$ data sets available for silicon. We have reproduced in Fig. 6(a) the $E_g(T)$ and $E_{gx}(T)$ data points given in Refs. 32 and 33, respectively. The simultaneous fit of both data sets using Eq. (23) gave the parameter values $\alpha = 3.23\times10^{-4}$ eV/K, $\Theta = 446$ K, and $\Delta = 0.51$ [in combination with a zero-temperature position of $E_g(0) = 1.1701$ eV for the fundamental band gap, and an extrapolated value of $E_{gx}(0) = 1.1564$ eV for the excitonic gap]. An alternative fit by Eq. (18) gave the same $T\rightarrow0$ positions with parameter values $\alpha = 3.15\times10^{-4}$ eV/K, $\Theta = 423$ K, and $\Delta = 0.50$. Comparing both parameter sets we notice differences of about 3%, 5%, and 2% between the magnitudes α, Θ, and Δ, respectively. Similarly small differences are also found with respect to earlier fittings of the same data [Fig. 6(a)] using the ρ-representation[6] or the two-oscillator model.[24] At the same time we must observe that, in contrast to the above requirement of $T_{\max}\gtrsim\Theta_D$, the experimental cut-off temperature[33] of $T_{\max} = 415$ K for the $E_{gx}(T)$ data set [cf. Fig. 6(a)] is considerably lower than the effective Debye temperature,[1] $\Theta_D \approx 670$ K, in Si. This means that, even with good agreement between fittings of different dispersion related models, the α and Θ values estimated hitherto can not yet be considered definitive.

The degree of uncertainty due to the limitation to $T \leqslant 415$ K of the $E_{gx}(T)$ data set of Ref. 33 can be estimated by examining other $E_{gx}(T)$ data sets for Si, e.g., in Refs. 59 and 60, which cover significantly higher temperatures. This is done in Figs. 6(b) and 6(c), in which we see that the total energy gap shift from 0 to 800 K amounts to about 0.18 eV and 0.20 eV. This corresponds to a difference of about 10% between the estimated magnitudes of limiting slopes α (Table II). According to Ref. 60, the magnitude of temperature variation of the gap was somewhat underestimated in

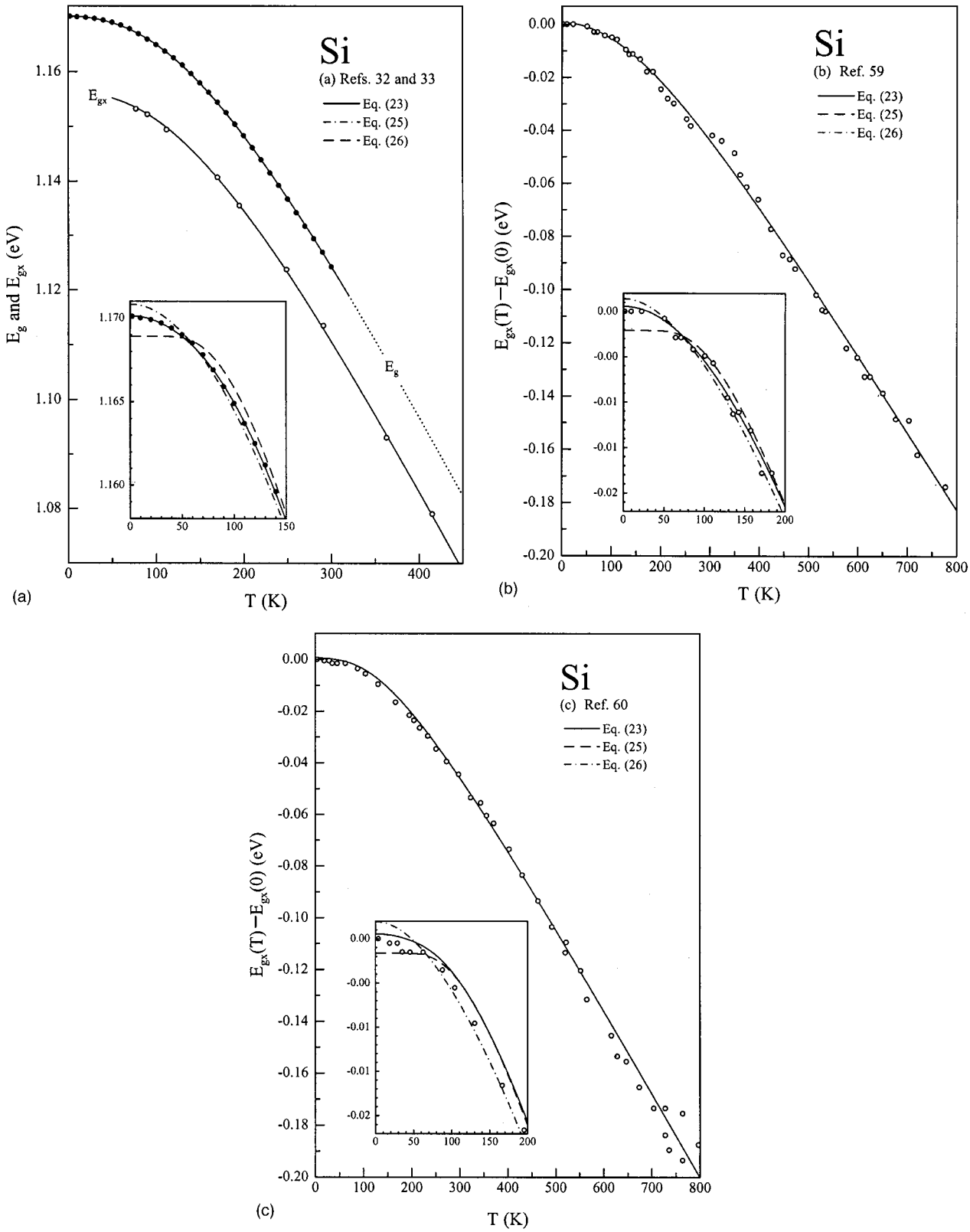

FIG. 6. Fittings of various $E(T)$ data sets available for silicon using Eq. (23). The insets show typical errors in the cryogenic region that arise from the Bose–Einstein model (25) and Varshni's formula (26). (a) Fundamental band gap data, $E_g(T)$, given by Bludau *et al.* (Ref. 32; dots) and excitonic gap data, $E_{gx}(T)$, given by Macfarlane *et al.* (Ref. 33; circles). (b) Excitonic gap shift data, $E_{gx}(0)-E_{gx}(T)$, given by Hartung *et al.* (Ref. 59). (c) Excitonic gap shift data, $E_{gx}(0)-E_{gx}(T)$, given by Alex *et al.* (Ref. 60).

TABLE II. Parameter sets obtained for silicon by fittings of the gap shift data of (a) Refs. 32 and 33 [cf. Fig. 6(a)], (b) Ref. 59 [cf. Fig. 6(b)], and (c) Ref. 60 [cf. Fig. 6(c)] using the dispersion-related four-parameter formula (23) compared with α_B and Θ_B values from the Bose–Einstein expression (25) and α_V and β values of Varshni's formula (26).

Refs.	Fig.	$\alpha/10^{-4}$ (eV/K)	Θ (K)	Δ	$\alpha_B/10^{-4}$ (eV/K)	Θ_B (K)	$\alpha_V/10^{-4}$ (eV/K)	β (K)
32, 33	6(a)	3.23	446	0.51	2.82	351	5.37	746
59	6(b)	3.02	440	0.61	2.87	381	3.36	357
60	6(c)	3.33	440	0.40	3.26	415	3.81	392

Ref. 59 [Fig. 6(b)] due to an insufficient line shape analysis procedure. One can see also from Fig. 6(c) that the α value detected from the data set of Ref. 60 has an uncertainty of about 5% due to the relatively large uncertainties (up to about 15 meV) of the experimental data in the region between 700 K and 800 K. The three different α values (Table II) taken from the three data sets of Figs. 6(a) to 6(c) yield thus the limiting slope in Si of about $\alpha \cong (3.2 \pm 0.2) \times 10^{-4}$ eV/K (with a remaining uncertainty of about 6%).

For the effective phonon temperature, Θ, we see from Table II that the estimated magnitudes are nearly the same for all three data sets. However, this approximate equality might be accidental. The above mentioned alternative fit of the data of Refs. 59 and 60 [Fig. 6(a)] using Eq. (18) gave a value of $\Theta = 423$ K (which is equal to that obtained by an earlier analysis using the ρ-representation[6]). Summarizing all the results for silicon, we come to an approximate value of $\Theta \cong (440 \pm 20)$ K for the effective phonon temperature. The associated dispersion coefficient amounts to $\Delta \cong (0.5 \pm 0.1)$ (Table II). The relatively large range of uncertainty in Δ is due to the scatter in the experimental points of Refs. 59 and 60 [insets to Figs. 6(b) and 6(c)] in the cryogenic region.

$E(T)$ data analyses performed using a dispersion-related (four-parameter) analytical model like the present one (Sec. III) are, as a rule, physically reasonable and numerically much more accurate than those applying a conventional (three-parameter) model like Varshni's formula[3,7] or a Bose–Einstein expression.[8–16] The latter represents the limiting case of completely vanishing dispersion, $\Delta \to 0$. It corresponds thus to a reduction of Eq. (23) to the limiting form[2,5]

$$E(T) \to E(0) - \frac{\alpha_B \Theta_B}{\exp(\Theta_B/T) - 1} = E(0) - \frac{\alpha_B \Theta_B}{2}\left[\coth\left(\frac{\Theta_B}{2T}\right) - 1\right]. \tag{25}$$

This model shows a *plateau* in the cryogenic region, $T < 50$ K, which is seen from the insets to Figs. 6(a) to 6(c) to be in clear *contradiction* to the approximately *quadratic* dependence, $(E(0) - E(T)) \propto T^2$ (24), observed in this region (not only for Si, but also for most other materials listed in Table I; cf. Ref. 5). From Table II we see that, for any one of the three data sets in consideration, the fitted magnitudes of the Bose–Einstein parameters, α_B and Θ_B, are considerably *smaller*, $\alpha_B < \alpha$ and $\Theta_B < \Theta$, than their dispersion-related counterparts α (3) and Θ (11). Note that the relative underestimation of the limiting slope, α, and of the effective phonon temperature, Θ, by Eq. (25) reaches 13% or 21%, respectively, for the data set in Fig. 6(a). (For a discussion of the analogous underestimation of both quantities for hexagonal GaN see Ref. 58.) Furthermore we see from Table II that the changes of α_B and Θ_B values from case to case [Figs. 6(a) to 6(c)] are considerably larger than the respective changes of the associated α and Θ values. This increase of parameter uncertainties arising from Eq. (25) [in comparison with Eqs. (23) or (18)] is plausible, in view of the obvious inadequacy of a model that assumes *vanishing* dispersion, $\Delta_B = 0$, especially when it is applied to a material like silicon that shows a relatively large degree of phonon dispersion, $\Delta \cong 0.5$ (cf. Tables I and II).

Consider finally Varshni's ad hoc formula,[3,7]

$$E_V(T) = E(0) - \frac{\alpha_V T^2}{\beta + T}. \tag{26}$$

Within this model, the parameter α_V should again represent the limiting slope, and the magnitude of the parameter β is commonly believed to be comparable[3,7] with the Debye temperature. (For a detailed analytical study of this model see Sec. V.) With respect to the low-temperature region of $T \ll \beta$ we see that $E_V(T)$ (26) tends to a *quadratic* asymptote[58]

$$E_V(T) \to E(0) - c_V T^2, \tag{27}$$

where $c_V \equiv \alpha_V/\beta$ represents the model-specific curvature coefficient [the counterpart to the coefficient c in Eq. (24)]. However, many numerical applications have shown that the magnitude of the dispersion-related curvature coefficient c (24) is (for $0 \leqslant \Delta \lesssim 3/4$, at least) significantly *smaller* than its counterpart c_V (27) associated with Varshni's parameter values α_V and β. This inequality between curvature coefficients, $c < c_V$, for the low temperature asymptotes, Eq. (24) vs Eq. (27), explains why experimental $E(T)$ data and calculated $E_V(T)$ curves in the cryogenic region almost never coincide [insets to Figs. 6(a) to 6(c)]. These systematic deviations are closely related to the enormous numerical uncertainties (instabilities) of Varshni's parameter values α_V and β. We see from Table II, e.g., that the α_V and β values for the data sets shown in Figs. 6(a) and 6(c) differ by factors of about 1.4 and 1.9, respectively (whereas the associated α and Θ values are nearly the same). Many least-mean-square fittings using Varshni's formula show a general tendency[5] of α_V and β values to be larger the lower the experimental cut-off temperature, $T_{\max}$, was chosen to be. Thus, these $\alpha_V(T_{\max})$ and $\beta(T_{\max})$ values are artificial, and cannot be considered as characteristic parameters of the physical system. In fact these

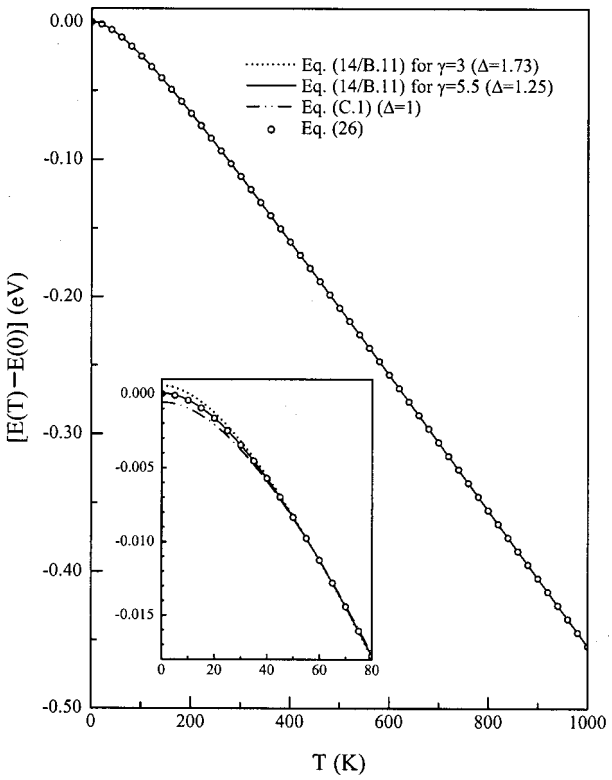

FIG. 7. Fittings of a set of hypothetical Varshni data points [following from Eq. (26) for $\alpha_V=5\times10^{-4}$ eV/K and $\beta=100$] using qualitatively different dispersion-related models. These models are represented, first, by Eq. (C1), which corresponds to the $\Delta=1$ limit of the analytical model developed in Sec. III (Appendix A) and, second, by Eq. (14) in combination with curve shape functions of type (B11), that represent a hypothetical regime of extremely large dispersion, $\Delta>1$ (see Appendices B and C).

physically unreasonable $T_{\max}$-dependencies can even lead to infinite α_V and β values, or a simultaneous change of both parameters to *negative* values, in cases[5,58] where $T_{\max}$ is significantly lower than half of the Debye temperature.

V. ASSESSMENT OF VARSHNI'S FORMULA

Let us give a physical explanation for the notorious inconsistency of Varshni's parameter values, based on the observation that Varshni's model corresponds to an unusually large degree of phonon dispersion, $\Delta_V>1$, which has never been found in experiment (cf. Table I). A preliminary estimate of the magnitude of the dispersion coefficient, Δ_V, associated with Varshni's *ad hoc* model[7] was made in Ref. 58. Choosing $\alpha_V=5\times10^{-4}$ eV/K and $\beta=100$ K for the parameters occurring in Varshni's formula (26) we have generated a series of sample $E(0)-E_V(T)$ data points (open circles in Fig. 7) for a temperature interval from 0 up to $10\beta=1000$ K. Least-mean-square fittings of these artificial Varshni data points were performed in Ref. 58 with two qualitatively different dispersion-related models, namely, the two-oscillator model[24] and the power law model.[20] Both fittings gave magnitudes for the dispersion coefficient of about unity, $\Delta_V\approx1$. However, it was also seen there that, particularly for the cryogenic region ($0<T<50$ K) which is crucial for a reliable determination of the dispersion coefficient, neither of these models provided an adequate fit. The systematic deviations in the cryogenic region (inset to Fig. 2 in Ref. 58) are because the two-oscillator model[24] tends to a plateau and the power law model[20] goes to a fractional power dependence,[58] $[E(0)-E(T)]\propto T^{1.4}$, while Varshni's model yields a quadratic low-temperature asymptote (27). Now, in contrast to the earlier models of Refs. 20 and 24, the dispersion-related models developed in the present study involve, for any $\Delta>0$, a *quadratic* low-temperature asymptote (24), the actual curvature of which increases monotonically with increasing Δ. The present analytical apparatus can thus be expected to permit a more adequate fit of hypothetical $E(0)-E_V(T)$ data points (cf. Fig. 7 and Appendix C) and a more correct determination of the dispersion coefficient, Δ_V, associated with Varshni's model (26).

Let us first estimate the magnitude of Δ_V analytically. To this end we compare the low- and high-temperature asymptotes of the present models (Sec. III and Appendices A and B) with those of Varshni's function (26). This allows us to ascertain parameter relationships that should assure coincidence of the respective asymptotes. Consider first the limiting region of *high* temperatures, $T\gg\Theta$, where the $E(T)$ dependences tend generally to *linear* asymptotes, namely: $E(T)\to E(0)-\alpha(T-\Theta/2)$, according to the dispersion-related theory [Eq. (13)], and $E_V(T)\to E(0)-\alpha_V(T-\beta)$, due to Varshni's model [Eq. (26)]. We see that both linear asymptotes are coincident just for[58]

$$\alpha_V=\alpha \quad \text{with} \quad \beta=\frac{\Theta}{2}. \tag{28}$$

Consider now the low-temperature asymptotes (24) and (27). These asymptotes are coincident when the corresponding curvature coefficients, $c\equiv\pi^2\Delta^2\alpha/(3(1+\Delta^2)\Theta)$ in Eq. (24) and $c_V\equiv\alpha_V/\beta$ in Eq. (27) have the same magnitude, i.e., for

$$c_V\equiv\frac{\alpha_V}{\beta}=\frac{2\alpha}{\Theta}=\frac{\pi^2\Delta^2\alpha}{3(1+\Delta^2)\Theta}\equiv c \tag{29}$$

[in accordance with Eq. (28)]. The latter relation is satisfied just for $\Delta^2/(1+\Delta^2)=6/\pi^2$, which corresponds to an effective magnitude for the dispersion coefficient of

$$\Delta\to\Delta_V=\left(\frac{\pi^2}{6}-1\right)^{-1/2}=1.2452. \tag{30}$$

The crucial feature of the latter result is due to a Δ_V value being even *significantly higher than unity* (at variance to the preliminary estimations[58] giving values of about unity).

Strictly speaking, the analytical model developed in Sec. III (Appendix A) was limited *a priori* to an interval of $0\leqslant\Delta<1$. This raises the question of whether, in view of the above use of the model-specific expression (24) for the low-temperature curvature coefficient, c, the resulting estimation (30) for the Varshni dispersion coefficient is internally consistent. To clarify this question we have considered in Appendix B a class of weighting functions $w_\gamma(\varepsilon)$ (B7) as representatives for a hypothetical regime of extremely large

dispersion, $\Delta>1$. Comparing the low- and high-temperature asymptotes of the corresponding (hypothetical) shape functions $\eta_{\gamma>2}(\xi)$ (B11) for $\Delta>1$ [i.e., Eqs. (B12) and (B13)], with those of the above considered shape functions $\eta_{\sigma>0}(\xi)$ (A6) for $0<\Delta<1$ [i.e., Eqs. (A7) and (A8), respectively] we see that the respective $\eta_\Delta(\xi)$ asymptotes are precisely the same. This proves the internal consistency of the above estimation (30) of the magnitude of Δ_V also within the analytical model developed in Appendix B for the corresponding (hypothetical) regime of extremely large dispersion, $\Delta>1$.

In order to realize that the estimated Δ_V value (30) reflects in adequate way not only the asymptotic behaviors of Varshni's hypothetical $E_V(T)$ curve (26) but applies, in fact, to *arbitrary* temperatures (starting from the cryogenic region, $0\leqslant T\ll\beta$, through the middle region, $T\approx\beta$, up to very high temperatures, $T\gg\beta$), we have performed in Appendix C a detailed numerical analysis (least-mean-square fit) of Varshni's hypothetical $E_V(T)$ curve (Fig. 7) using the analytical model developed in Appendix B for the hypothetical regime of extremely large dispersion ($\Delta>1$). As a final result of this detailed *numerical* analyses (in Appendix C) we have obtained a value of $\Delta_V=1.2535$, which deviates from the *analytical* value (30) by only about 0.7%. Thus a magnitude of about $\Delta_V\cong1.25$ (within an uncertainty lesser than ±0.01) can be considered as a definitive value for the dispersion coefficient associated with Varshni's formula (26).[3,7]

VI. CONCLUSIONS

In summary we can say that Varshni's model (26) assumes an *extremely large* degree of phonon dispersion, which is unrealistic based on detailed least-mean-square fittings of experimental data sets, $0\leqslant\Delta\lesssim3/4$. This applies not only to the group IV, III–V, and II–VI materials considered in this article. In fact, in the large number of available experimental $E(T)$ data sets for different classes of binary and ternary semiconductor materials (in bulk) or heterostructures, no indication of very large dispersion, $\Delta>1$, could ever be found. Thus, there is hardly a chance for Varshni's *ad hoc* model to give a physically reasonable interpretation of the gap shrinkage effect in such a system. Sample analyses, e.g.,[61] of the exciton energy data given by Mudryi *et al.*[62] for $ZnAs_2$, of the photoluminescence peak positions given by Tu *et al.*[63] for a $Ga_2O_3(Gd_2O_3)$ thin film, or of the excitonic peak position data given by Homs and Marí[64] for the layered III–VI material InSe, have shown that these are associated with the regime of *moderate* (intermediate) dispersion,[6] $0.3<\Delta<0.5$ (as are the majority of the materials listed in Table I). Thus in view of the much larger dispersion coefficient $\Delta_V\cong1.25$ (30) of Varshni's model (26) and the vanishing dispersion coefficient, $\Delta_B=0$, for the Bose–Einstein model (25), neither of these conventional three-parameter models is capable of providing physically adequate interpretations of $E(T)$ dependences. In contrast, the novel four-parameter expression (23), owing to its large range of applicability, $0\leqslant\Delta\lesssim3/4$, is found to be well suited for numerical analyses of $E(T)$ data sets for a large variety of binary and ternary semiconductor materials and heterostructures. Corresponding sample analyses will be published in forthcoming papers.

APPENDIX A: MODEL FOR SMALL TO LARGE DISPERSION ($0\leqslant\Delta<1$)

Consider a class of weighting functions of type

$$w_\sigma(\varepsilon)=\frac{\sigma}{\varepsilon_o}\cdot\left(1-\frac{\varepsilon}{\varepsilon_o}\right)^{\sigma-1},\quad \sigma>0, \tag{A1}$$

for ε up to a certain cut-off energy, $0\leqslant\varepsilon\leqslant\varepsilon_o$, and $w_\sigma(\varepsilon)=0$ elsewhere (Fig. 1). The calculation of the corresponding model-specific moments (10) involves certain definite integrals of which the analytical solutions are known from standard mathematical literature to be given by

$$\int_0^1 x^m(1-x)^{\sigma-1}dx=\frac{\Gamma(\sigma)\Gamma(m+1)}{\Gamma(\sigma+m+1)} \tag{A2}$$

[where $\Gamma(m+1)=m!$, for $m=0,1,2,...$]. In accordance with the standard relation $\Gamma(z+1)=z\cdot\Gamma(z)$ for Γ-functions we obtain thus for the model-specific moments (10)

$$\langle\varepsilon^m\rangle=\frac{m!\varepsilon_o^m}{(\sigma+m)\cdot(\sigma+m-1)\cdot\ldots\cdot(\sigma+1)}. \tag{A3}$$

This expression reduces to $\langle\varepsilon\rangle=\varepsilon_o/(\sigma+1)$ and $\langle\varepsilon^2\rangle=2\varepsilon_o^2/((\sigma+1)(\sigma+2))$, for the first and second moment, respectively. The dispersion coefficient (12) is thus given in terms of the curve shape parameter $\sigma>0$ by

$$\Delta=\sqrt{\frac{\sigma}{\sigma+2}},\ \text{i.e., conversely}\ \sigma=\frac{2\Delta^2}{1-\Delta^2}, \tag{A4}$$

and the effective phonon temperature Eq. (11) is related to $\Theta_o\equiv\varepsilon_o/k_B$ by

$$\Theta=\frac{1}{\sigma+1}\Theta_o=\frac{1-\Delta^2}{1+\Delta^2}\Theta_o \tag{A5}$$

[in accordance with Eq. (A4)]. The relative simplicity of relationships (A4) and (A5) between the auxiliary quantities Θ_o and σ, on the one hand, and the basic dispersion-related parameters Θ and Δ, on the other hand, enables us to represent the final results directly in terms of the latter [cf. point (4) quoted in Sec. I].

Inserting the model function $w_\sigma(\varepsilon)$ (A1) into Eq. (5) and including Eq. (A5) we can write the $E(T)$ dependence (5) in a general form (14), where the characteristic (dimensionless) shape function η is defined, in terms of the dimensionless ratio $\xi\equiv2T/\Theta$ and the parameter $\sigma>0$, by integrals of the form

$$\eta_\sigma(\xi)\equiv2\sigma(\sigma+1)\int_0^1 dx\,\frac{x(1-x)^{\sigma-1}}{\exp\left(\frac{2(\sigma+1)}{\xi}x\right)-1}$$
$$\equiv\frac{\sigma}{2(\sigma+1)}\xi^2\int_0^{2(\sigma+1)/\xi}dz\,\frac{z\left(1-\frac{\xi z}{2(\sigma+1)}\right)^{\sigma-1}}{\exp(z)-1}. \tag{A6}$$

The latter representation shows that, due to the rapid increase of the exponential $\exp(z)$ (in the second representation), more than 95% of the resulting value of the integral comes from the interval $0<z<5$. Within this interval, for sufficiently *low* temperatures, $\xi/(\sigma+1)\ll 1$, the term $\xi z/[2(\sigma+1)]$ is much smaller than unity. Neglecting hence this term and extending the range of integration to infinity we come to a limiting value of $\pi^2/6$ [=Eq. (7) for $n=0$] for the integral occurring in the second representation of Eq. (A6). The corresponding (quadratic) low-temperature asymptote is thus given by

$$\eta_\sigma(\xi)\rightarrow \frac{\pi^2\sigma}{12(\sigma+1)}\xi^2=\frac{\pi^2\Delta^2}{6(1+\Delta^2)}\xi^2\equiv\eta_\Delta(\xi\ll 1) \tag{A7}$$

[the latter equality being in accordance with Eq. (A4)].

For sufficiently *high* temperatures, $z\equiv 2(\sigma+1)x/\xi\leqslant 2(\sigma+1)/\xi<2\pi$, we can make use of the Taylor expansion $z/[\exp(z)-1]=1-z/2+z^2/12-\ldots$. Taking the known solutions for the three lowest-order integrals ($m=0$, 1, and 2) of type (A2), we come to an intermediate-to-high temperature expression for the characteristic shape function of the form

$$\eta_\sigma(\xi)\rightarrow\xi-1+\frac{2(\sigma+1)}{3(\sigma+2)\xi}=\xi-1+\frac{1+\Delta^2}{3\xi}\equiv\eta_\Delta(\xi\gg 1) \tag{A8}$$

[in accordance again with Eq. (A4)].

Consider further the problem of reliable *numerical* calculations of the shape function $\eta_\sigma(\xi)$ (A6) for any ξ [i.e., in particular for the middle region, $\pi<(\sigma+1)/\xi<10$, where the $\eta_\sigma(\xi)$ dependence deviates significantly from asymptotes (A7) and (A8)]. From Eq. (A4) we see that for moderate (small to intermediate) dispersion, $0<\Delta<\Delta_c=3^{-1/2}$, the parameter σ ranges within the interval $0<\sigma<1$. The corresponding weighting functions $w_\sigma(\varepsilon)$ (A1) are monotonically *increasing* with increasing phonon energy ε and have a *singularity* at $\varepsilon\rightarrow\varepsilon_o$ (cf. Fig. 1). This corresponds to a singularity of the factor $(1-x)^{\sigma-1}$ in Eq. (A6) (in the first version of integral representations) for the characteristic shape function, $\eta_\sigma(\xi)$, at the upper end, $x\rightarrow 1$, of the integration interval. Consequently, the representation (A6) cannot be used for numerical integration in cases of moderate (small and intermediate) dispersion, $0<\Delta<3^{-1/2}$. For the sake of reliable numerical calculations of integrals of type (A6) it is thus necessary to bring the upper section of these integrals, by an integration by parts, into a form where the transformed integrands are finite everywhere (vanishing at $x\rightarrow 1$).

Let us denote by x_c a point ranging somewhere in the middle region between the lower and upper boundaries of integration, $0<x_c<1$ (e.g., $x_c\rightarrow 0.5$), in Eq. (A6), and consider the total integral (A6) as a sum of two partial integrals for the sections $0\leqslant x\leqslant x_c$ and $x_c\leqslant x\leqslant 1$, respectively. For the sake of a convenient transformation of the second integral by parts we introduce the auxiliary functions

$$u(x)\equiv(1-x)^\sigma \quad\text{and}\quad \nu(x)\equiv\frac{x}{\exp(2(\sigma+1)x/\xi)-1}. \tag{A9}$$

Their first derivatives are given by

$$u'(x)=-\sigma(1-x)^{\sigma-1} \quad\text{and}\quad \nu'(x)=\frac{1}{\exp(2(\sigma+1)x/\xi)-1} - \frac{(\sigma+1)x}{2\xi(\sinh(2(\sigma+1)x/\xi))^2}. \tag{A10}$$

Evaluating, henceforth, the second integral by parts,

$$\int_{x_c}^1 dx\ \ u'(x)\nu(x)=[u(x)\nu(x)]_{x_c}^1-\int_{x_c}^1 dx\ \ u(x)\nu'(x) \tag{A11}$$

we obtain for the total integral (A6) an expression of the form

$$\eta_\sigma(\xi)=2(\sigma+1)\left\{\sigma\int_0^{x_c}dx\,\frac{x(1-x)^{\sigma-1}}{\exp(2(\sigma+1)x/\xi)-1} + \frac{x_c(1-x_c)^\sigma}{\exp(2(\sigma+1)x_c/\xi)-1} + \int_{x_c}^1 dx\,\frac{(1-x)^\sigma}{\exp(2(\sigma+1)x/\xi)-1} - \frac{(\sigma+1)}{2\xi}\int_{x_c}^1 dx\,\frac{x(1-x)^\sigma}{(\sinh(2(\sigma+1)x/\xi))^2}\right\}. \tag{A12}$$

The integrands in these partial integrals are seen to be free from singularities (for any $\sigma>0$). Thus the latter representation (A12) is suitable for numerical calculations of shape functions, $\eta_\sigma(\xi)$, within the whole region of dispersion coefficients, $0<\Delta<1$ Eq. (A4), associated with the model function $w_\sigma(\varepsilon)$ (A1) in consideration.

APPENDIX B: MODELS FOR EXTREMELY LARGE DISPERSION ($\Delta\geqslant 1$)

Let us consider first the $\sigma\rightarrow\infty$ limit of the analytical model displayed in Sec. III which, according to Eq. (A4), should correspond just to a magnitude of $\Delta\rightarrow 1$ for dispersion coefficient. Within this model, the cut-off energy ε_o [in Eq. (A1)] can be represented in terms of the parameter $\sigma>0$ and the associated average phonon energy $\langle\varepsilon\rangle$ as $\varepsilon_o=(\sigma+1)\langle\varepsilon\rangle$ [in accordance with Eq. (A3)]. Consequently we can rewrite the weighting function $w_\sigma(\varepsilon)$ (A1) in the equivalent form

$$w_\sigma(\varepsilon)=\frac{\sigma}{(\sigma+1)\langle\varepsilon\rangle}\left(1-\frac{\varepsilon}{(\sigma+1)\langle\varepsilon\rangle}\right)^{\sigma-1}. \tag{B1}$$

Referring to the well-known representation of exponential functions by limits of type

$$\lim_{p\rightarrow\infty}(1\mp x/p)^{\pm p}=\exp(-x), \tag{B2}$$

where $x=\varepsilon/\langle\varepsilon\rangle$ and the parameter p differs from the corresponding quantities $\sigma\pm 1$ in Eq. (B1) by only ± 1 (this dif-

ference being negligible in the $\sigma\to\infty$ limit), we see that Eq. (B1) goes to the exponential function

$$w_{\Delta=1}(\varepsilon)\equiv w_{\sigma\to\infty}(\varepsilon)=\frac{1}{\langle\varepsilon\rangle}\exp\left(-\frac{\varepsilon}{\langle\varepsilon\rangle}\right),\quad 0\leqslant\varepsilon<\infty. \tag{B3}$$

The latter is again properly normalized (to unity) and the moments (10) are $\langle\varepsilon^m\rangle=m!\langle\varepsilon\rangle^m$, i.e., in particular $\langle\varepsilon^2\rangle=2\langle\varepsilon\rangle^2$, for the second moment. This result confirms [according to Eq. (12)] the value indicated above for the associated dispersion coefficient, $\Delta=1$.

Inserting Eq. (B3) into Eq. (5) and representing the average phonon energy as usual in terms of the phonon temperature, $\Theta=\langle\varepsilon\rangle/k_B$ (11), we obtain for the $E(T)$ dependence again an expression of the general form (14), where the dependence of the corresponding shape function $\eta_{\Delta=1}$ on the dimensionless argument $\xi\equiv 2T/\Theta$ is given by integrals of the form

$$\eta_{\Delta=1}(\xi)\equiv 2\int_0^{(\infty)}dx\,\frac{x\exp(-x)}{\exp\left(\frac{2x}{\xi}\right)-1}$$

$$=\frac{1}{2}\xi^2\int_0^{(\infty)}dz\,\frac{z\exp\left(-\frac{\xi z}{2}\right)}{\exp(z)-1}. \tag{B4}$$

Representing the Bose–Einstein factor in the latter integral by the expansion

$$(\exp(z)-1)^{-1}=\sum_{n=1}^{\infty}\exp(-nz) \tag{B5}$$

(which is convergent for any $z>0$), we can readily perform the integration for the individual $\exp(-nz)$ terms. In this way we transform the shape function $\eta_{\Delta=1}(\xi)$ (B4) *exactly* into a series expansion of the form

$$\eta_{\Delta=1}(\xi)=\frac{1}{2}\xi^2\sum_{n=1}^{\infty}\frac{1}{\left(n+\frac{\xi}{2}\right)^2}. \tag{B6}$$

A series of numerical values is represented by the squares in Fig. 2. Comparing these $\eta_{\Delta=1}(\xi)$ values with Varshni's characteristic shape function, $\eta_V(\xi)=\xi^2/(\xi+1)$ (Fig. 2), we see that the latter shows an even *stronger* curvature than $\eta_{\Delta=1}(\xi)$ (B6). This is an indication for the effective dispersion coefficient associated with Varshni's model (26) to be somewhat *higher* than unity, $\Delta_V>1$. For a more accurate estimation of Δ_V we need, consequently, an analytical model applying to a (hypothetical) regime of extremely large dispersion, $\Delta>1$.

A convenient choice for an analytical $\Delta>1$ model, which can be looked upon as a natural extension of the model function $w_\sigma(\varepsilon)$ (A1) considered above (for $0<\Delta<1$, in Appendix A and Secs. III and IV), is given by a weighting function of type

$$w_\gamma(\varepsilon)=\frac{\gamma}{\varepsilon_o}\cdot\left(1+\frac{\varepsilon}{\varepsilon_o}\right)^{-\gamma-1},\quad\text{where}\quad\gamma>2. \tag{B7}$$

Observing that

$$\int_0^\infty\frac{x^m}{(1+x)^{\gamma+1}}dx=\frac{\Gamma(\gamma-m)\Gamma(m+1)}{\Gamma(\gamma+1)},\quad\text{for}\quad -1<m<\gamma, \tag{B8}$$

we see that the two nontrivial lowest-order moments (10) are $\langle\varepsilon\rangle=\varepsilon_o/(\gamma-1)$ and $\langle\varepsilon^2\rangle=2\varepsilon_o^2/((\gamma-1)(\gamma-2))$. The dispersion coefficient (12) is thus given in terms of the curve shape parameter $\gamma>2$ by

$$\Delta=\sqrt{\frac{\gamma}{\gamma-2}},\quad\text{i.e., conversely}\quad\gamma=\frac{2\Delta^2}{\Delta^2-1}, \tag{B9}$$

and the effective phonon temperature (11) is related to $\Theta_o\equiv\varepsilon_o/k_B$ by equation

$$\Theta=\frac{1}{\gamma-1}\Theta_o=\frac{\Delta^2-1}{\Delta^2+1}\Theta_o. \tag{B10}$$

Inserting the model function (B7) into Eq. (5) and observing Eq. (B10) we can write the $E(T)$ dependence (5) again in the general form (14) with a characteristic shape function η, however, that is given now by (equivalent) integrals of the form

$$\eta_\gamma(\xi)\equiv 2\gamma(\gamma-1)$$

$$\times\int_0^\infty dx\,\frac{x}{(1+x)^{\gamma+1}\left[\exp\left(\frac{2(\gamma-1)}{\xi}x\right)-1\right]}$$

$$=\frac{\gamma}{2(\gamma-1)}\xi^2\int_0^{(\infty)}dz\,\frac{z}{\left(1+\frac{\xi z}{2(\gamma-1)}\right)^{\gamma+1}[\exp(z)-1]}. \tag{B11}$$

The second representation of $\eta_\gamma(\xi)$ shows [in analogy to the counterpart for $\eta_\sigma(\xi)$ in Eq. (A6)] that, due to the rapid increase of the exponential, $\exp(z)$, more than 95% of the resulting value of the integral comes from the interval $0<z<5$. Within this interval, for sufficiently *low* temperatures [(i.e., here $(\gamma-1)/\xi>10$), the term $\xi z/(2(\gamma-1))$] is small compared to unity. Neglecting this term we come again to a limiting value of $\pi^2/6$ [=Eq. (7) for $n=0$] for the integral occurring in the second representation of Eq. (B11). The corresponding (quadratic) low-temperature asymptote reads thus, explicitly,

$$\eta_\gamma(\xi)\to\frac{\pi^2\gamma}{12(\gamma-1)}\xi^2=\frac{\pi^2\Delta^2}{6(1+\Delta^2)}\xi^2\equiv\eta_{\Delta>1}(\xi\ll 1) \tag{B12}$$

[in accordance with Eq. (B9)]. An important feature of Eq. (B12), particularly with respect to the analytical study in Sec. V, is the perfect coincidence of the asymptote $\eta_{\Delta>1}(\xi\ll 1)$ (B12) for the hypothetical regime of extremely large disper-

sion with its counterpart $\eta_{0<\Delta<1}(\xi \ll 1)$ (A7) for the physically realistic regimes of small to moderately large dispersion (Secs. III and IV).

For sufficiently *high* temperatures, $z \equiv 2(\gamma-1)x/\xi \leqslant 2(\gamma-1)/\xi < 2\pi$, we can again make use of the Taylor expansion $z/[\exp(z)-1]=1-z/2+z^2/12-\ldots$. Substituting the parameter $\gamma>2$ by the corresponding dispersion coefficient Δ [according to Eq. (B8)] we come, formally, again to an asymptotic shape function expression of the usual form (A8),

$$\eta_\gamma(\xi) \rightarrow \xi - 1 + \frac{2(\gamma-1)}{3(\gamma-2)\xi} = \xi - 1 + \frac{1+\Delta^2}{3\xi} \equiv \eta_{\Delta>1}(\xi \gg 1). \tag{B13}$$

We wish to point out that, within the frame of this *hypothetical* model for extremely large dispersion, $\Delta>1$, it is not possible to construct a complete high-temperature series expansion in analogy to Eq. (9) by adding further ξ^{-n} terms, $n=3,5,7,...$, to Eq. (B13). This is due to the fact that, depending on the actual magnitude of the parameter $2<\gamma<+\infty$, the corresponding higher-order moments $\langle \varepsilon^m \rangle$, $m>\gamma$, tend to infinity.

APPENDIX C: DISPERSION-RELATED FIT OF VARSHNI'S HYPOTHETICAL $E(T)$ FUNCTION

First of all we can clearly exclude the eventuality of a Δ_V value lower than unity, e.g., by performing a numerical fit of the hypothetical $E(0)-E_V(T)$ data points (Fig. 7) on the basis of the model developed in Appendix A (Sec. III). Using Eq. (14) for the $E(T)$ dependence along with the exact (integral) representation (A6) for the characteristic shape function, $\eta_\sigma(\xi) \equiv \eta_\sigma(2T/\Theta)$, we are concerned with a least-mean-square process involving an unlimited increase of the curve shape parameter, $\sigma \rightarrow \infty$. The latter corresponds, according to Eq. (A4), to an approach of the dispersion coefficient just to unity,[58] $\Delta \rightarrow 1$. In this limit (see Appendix B), the weighting function $w_\sigma(\varepsilon)$ (A1) reduces to an exponential, $w_{\Delta=1}(\varepsilon) \propto \exp(-\varepsilon/\langle\varepsilon\rangle)$ (B3). The latter enables a transformation of the integral (B4) for the corresponding shape function, $\eta_{\Delta=1}(\xi)$, into a series expansion (B6). From the latter follows, in combination with Eq. (14), for the $E(T)$ dependence in this special case a series expansion of the relatively simple form

$$E_{\Delta=1}(T) = E(0) - \frac{\alpha T^2}{\Theta} \sum_{n=1}^{\infty} \left(n + \frac{T}{\Theta} \right)^{-2}. \tag{C1}$$

This expression is exact [with respect to the limiting weighting function (B3)] and is convergent for any T. Performing a least-mean-squares fitting of the $E(0)-E_V(T)$ data points (Fig. 7) using the three-parameter expression (C1) we have obtained the parameter values $\alpha = 4.971 \times 10^{-4}$ and $\Theta = 186.2$ K. [Note that these values are nearly equal to those obtained in Ref. 58 from a fitting of the same set of $E(0)-E_V(T)$ data points by the two-oscillator model.[24]] The corresponding ratios $\alpha_V/\alpha = 1.006$ and $\beta/\Theta = 0.537$ between the α_V and β values chosen above and the fitted α and Θ values are in reasonable agreement with analytical relations (28). At the same time we see from the inset to Fig. 7 that the fitted $E_{\Delta=1}(T)$ curve (C1) tends to a $E_{\Delta=1}(T \rightarrow 0)$ limiting position which is located about 0.58 meV *below* the original $E_V(T \rightarrow 0)$ position of the Varshni curve. A small deviation like this might appear to be almost negligible in experiment, since experimental uncertainties, even in the $T \rightarrow 0$ limit, are often of the same order. However, we also see from the inset to Fig. 7 that the curvature of the $E_V(T)$ curve in the cryogenic region ($0<T<50$ K) is about 14% stronger than that of the $E_{\Delta=1}(T)$ curve (C1). Thus we are concerned again with *systematic* deviations indicating that the effective dispersion coefficient Δ_V associated with Varshni's model must be at least *larger* than unity, $\Delta_V > 1$.

We have considered in Appendix B a class of weighting functions $w_\gamma(\varepsilon)$ (B7) for extremely large dispersion, $\Delta>1$, which have the convenient property of approaching in the $\gamma \rightarrow \infty$ limit the same (exponential) function (B3) as the previous weighting function $w_\sigma(\varepsilon)$ (A1) (Sec. III) in the $\sigma \rightarrow \infty$ limit. This choice (B7) assures automatically a *continuous* change of fitted α and Θ values when we pass from the physically relevant dispersion region $0<\Delta<1$ to the hypothetical region $\Delta>1$. Taking hence the shape function $\eta(\xi)$ for the $E(T)$ dependence [in Eq. (14)] in the form of the integral representation $\eta_\gamma(\xi)$ (B11) and fixing preliminarily the shape parameter to $\gamma=3$ we have performed a three-parameter fit of the same $E(0)-E_V(T)$ data points (Fig. 7). The resulting parameter values are $\alpha = 5.026 \times 10^{-4}$ and $\Theta = 213.4$ K. The corresponding ratios $\alpha_V/\alpha = 0.995$ and $\beta/\Theta = 0.469$ are again in good agreement with analytical relations (28). Comparing the latter parameter ratios for fixed $\gamma=3$ [which corresponds to a dispersion coefficient of $\Delta = 3^{1/2} \cong 1.73$ (B9)] with those quoted above for fixed $\Delta=1$ we see that their relative deviations from the theoretical ideal values of $\alpha_V/\alpha = 1$ and $\beta/\Theta = 0.5$ (28) have nearly the *same magnitude*, namely of about $\pm 0.6\%$ for α and $\pm 7\%$ for Θ. Of special importance is the finding, however, that these model-specific deviations of parameter ratios have *opposite signs* for these two alternative fits. An analogous statement can also be made with respect to the deviations of fitted $E(T \rightarrow 0)$ limiting positions from the original $E_V(T \rightarrow 0)$ position of the Varshni curve. In the case of the $\gamma=3$ ($\Delta = 3^{1/2}$) the $E(T \rightarrow 0)$ position is located about 0.55 meV *above* $E_V(T \rightarrow 0)$ (cf. Fig. 7). Thus the model-specific deviations of fitted $E(T \rightarrow 0)$ positions from the $E_V(T \rightarrow 0)$ position are found to have nearly the *same* magnitude ($\cong 0.6$ meV), but *opposite* sign, for the $\Delta = 3^{1/2}$ vs $\Delta=1$ fit (cf. Fig. 7). These results of the two alternative three-parameter fits suggest that the effective value of the Varshni dispersion coefficient should be located somewhere between these fixed Δ values, i.e., at least $1 < \Delta_V < 3^{1/2}$ [in qualitative agreement with Eq. (30)].

Finally, for a more conclusive determination of Δ_V we have performed a complete four-parameter fit [using again Eq. (14) in combination with Eq. (B11)]. The corresponding least-mean-square fitting procedure resulted in a dramatic *order-of magnitude decrease* of the residual variance (namely, by factors of about 340 or 230 in comparison with those left by the three-parameter fits for $\Delta=1$ and $\Delta = 3^{1/2}$,

respectively). Consequently we are concerned with an extremely fine dispersion-related fit (Fig. 7) which is almost indistinguishable from Varshni's original $E_V(T)$ data set. [Note that the maximum deviation between the given $E_V(T)$ data set and the fitted $E(T)$ curve, which occurs at $T \rightarrow 0$, amounts to only 0.036 meV. Note further that the standard deviation is even somewhat smaller than 0.01 meV]. The associated parameter values are $\alpha = 4.9955 \times 10^{-4}$ and $\Theta = 196.12$ K with $\gamma = 5.501$. This means, among other things, a much closer approach than before of the associated parameter ratios, $\alpha_V / \alpha = 1.0009$ and $\beta/\Theta = 0.51$, to their ideal (theoretical) magnitudes of 1 and 1/2 Eq. (28). At the same time we infer from Eq. (B9) that a fitted magnitude of $\gamma = 5.501$ corresponds to a dispersion coefficient of $\Delta_V = 1.2535$. The latter deviates from the ideal (theoretical) magnitude (30) by only about 0.7%.

*Electronic address: passler@physik.tu-chemnitz.de

[1] O. Madelung (Ed.), Landolt-Börnstein: ''Numerical Data and Functional Relationships in Science and Technology,'' Group III, Vols. 17a and 22a (Springer, Berlin, 1982 and 1989).

[2] R. Pässler, Phys. Status Solidi B **200**, 155 (1997).

[3] C. D. Thurmond, J. Electrochem. Soc. **122**, 1133 (1975).

[4] R. Pässler, Solid-State Electron. **39**, 1311 (1996).

[5] R. Pässler, Phys. Status Solidi B **216**, 975 (1999).

[6] R. Pässler, J. Appl. Phys. **88**, 2570 (2000).

[7] Y. P. Varshni, Physica (Amsterdam) **34**, 149 (1967).

[8] G. D. Cody, in *Hydrogenated Amorphous Silicon*, edited by J. I. Pankove, Semiconductors and Semimetals (Academic, New York, 1984), Vol. 21 (b), Chap. 2, pp. 11–79.

[9] A. Manoogian and J. C. Woolley, Can. J. Phys. **62**, 285 (1984).

[10] L. Viña, S. Logothetidis, and M. Cardona, Phys. Rev. B **30**, 1979 (1984).

[11] S. Logothetidis, L. Viña, and M. Cardona, Phys. Rev. B **31**, 947 (1985).

[12] P. Lautenschlager, M. Garriga, S. Logothetidis, and M. Cardona, Phys. Rev. B **35**, 9174 (1987).

[13] K. P. O'Donnell and X. Chen, Appl. Phys. Lett. **58**, 2924 (1991).

[14] S. Zollner, M. Garriga, J. Kircher, J. Humlíček, and M. Cardona, Phys. Rev. B **48**, 7915 (1993).

[15] K. P. Korona, A. Wysmołek, K. Pakuła, R. Stępniewski, J. M. Baranowski, I. Grzegory, B. Łucznik, M. Wróblewski, and S. Porowski, Appl. Phys. Lett. **69**, 788 (1996).

[16] Kuan-Cheng Chiu, Yu-Ching Su, and Hang-An Tu, Jpn. J. Appl. Phys. **37**, Pt. 1, 6374 (1998).

[17] R. Pässler, F. Blaschta, E. Griebl, K. Papagelis, B. Haserer, T. Reisinger, S. Ves, and W. Gebhardt, Phys. Status Solidi B **204**, 685 (1997).

[18] S. A. Lourenço, I. F. L. Dias, J. L. Duarte, E. Laureto, E. A. Meneses, J. R. Leite, and I. Mazzaro, J. Appl. Phys. **89**, 6159 (2001).

[19] R. Pässler and G. Oelgart, J. Appl. Phys. **82**, 2611 (1997).

[20] R. Pässler, J. Appl. Phys. **83**, 3356 (1998).

[21] S. A. Lourenço, I. F. L. Dias, J. L. Duarte, E. Laureto, H. Iwamoto, E. A. Meneses, and J. R. Leite, Superlattices Microstruct. **29**, 225 (2001).

[22] S. A. Lourenço, I. F. L. Dias, E. Laureto, J. L. Duarte, D. O. Toginho Filho, E. A. Meneses, and J. R. Leite, Eur. Phys. J. B **21**, 11 (2001).

[23] S. Martini, A. A. Quivy, A. Tabata, and J. R. Leite, J. Appl. Phys. **90**, 2280 (2001).

[24] R. Pässler, J. Appl. Phys. **89**, 6235 (2001).

[25] E. Antončík, Czech. J. Phys., Sect. B **5**, 449 (1955).

[26] H. D. Vasileff, Phys. Rev. **105**, 441 (1957).

[27] E. N. Adams, Phys. Rev. **107**, 671 (1957).

[28] D. G. Seiler, J. R. Lowney, C. L. Littler, and I. T. Yoon, Mater. Res. Soc. Symp. Proc. **216**, 59 (1991).

[29] A. Göbel, T. Ruf, M. Cardona, C. T. Lin, J. Wrzesinski, M. Steube, K. Reimann, J.-C. Merle, and M. Joucla, Phys. Rev. B **57**, 15 183 (1998).

[30] C. D. Clark, P. J. Dean, and P. V. Harris, Proc. R. Soc. London, Ser. A **277**, 312 (1964).

[31] L. Patrick, D. R. Hamilton, and W. J. Choyke, Phys. Rev. **132**, 2023 (1963).

[32] W. Bludau, A. Onton, and W. Heinke, J. Appl. Phys. **45**, 1846 (1974).

[33] G. G. Macfarlane, T. P. McLean, J. E. Quarrington, and V. Roberts, Phys. Rev. **111**, 1245 (1958).

[34] G. G. Macfarlane, T. P. McLean, J. E. Quarrington, and V. Roberts, J. Phys. Chem. Solids **8**, 388 (1959).

[35] D. Brunner, H. Angerer, E. Bustarret, F. Freudenberg, R. Höpler, R. Dimitrov, O. Ambacher, and M. Stutzmann, J. Appl. Phys. **82**, 5090 (1997).

[36] B. Monemar, Phys. Rev. B **8**, 5711 (1973).

[37] C. Alibert, A. Joullié, A. M. Joullié, and C. Ance, Phys. Rev. B **27**, 4946 (1983).

[38] H. Herr, Diplomarbeit, Technical University München, 1996.

[39] P. J. Dean, G. Kaminsky, and R. B. Zetterstrom, J. Appl. Phys. **38**, 3551 (1967).

[40] M. R. Lorenz, G. D. Pettit, and R. C. Taylor, Phys. Rev. **171**, 876 (1968).

[41] E. Grilli, M. Guzzi, R. Zamboni, and L. Pavesi, Phys. Rev. B **45**, 1638 (1992).

[42] M. B. Panish and H. C. Casey, Jr., J. Appl. Phys. **40**, 163 (1969).

[43] M. Shah, M. O. Manasreh, R. Kaspi, M. Y. Yen, B. A. Philips, M. Skowronski, and J. Shinar, Mater. Res. Soc. Symp. Proc. **325**, 449 (1994).

[44] C. Ghezzi, R. Magnanini, A. Parisini, B. Rotelli, L. Tarricone, A. Bosacchi, and S. Franchi, Phys. Rev. B **52**, 1463 (1995).

[45] Q. Guo and A. Yoshida, Jpn. J. Appl. Phys. **33**, Pt. 1, 2453 (1994).

[46] L. Pavesi, F. Piazza, A. Rudra, J. F. Carlin, and M. Ilegems, Phys. Rev. B **44**, 9052 (1991).

[47] Z. Hang, H. Shen, and F. H. Pollak, Solid State Commun. **73**, 15 (1990).

[48] Z. M. Fang, K. Y. Ma, D. H. Jaw, R. M. Cohen, and G. B. Stringfellow, J. Appl. Phys. **67**, 7034 (1990).

[49] P. Y. Liu and J. C. Maan, Phys. Rev. B **47**, 16 279 (1993).

[50] R. Pässler, E. Griebl, H. Riepl, G. Lautner, S. Bauer, H. Preis, W. Gebhardt, B. Buda, D. J. As, D. Schikora, K. Lischka, K. Papagelis, and S. Ves, J. Appl. Phys. **86**, 4403 (1999).

[51] D. G. Thomas and J. J. Hopfield, Phys. Rev. **116**, 573 (1959).

[52] C. B. à la Guillaume, J.-M. Debever, and F. Salvan, Phys. Rev. **177**, 567 (1969).

[53] A. Anedda and E. Fortin, Phys. Status Solidi A **36**, 385 (1976).

[54] D. G. Seiler, D. Heiman, R. Feigenblatt, R. L. Aggarwal, and B.

Lax, Phys. Rev. B **25**, 7666 (1982).
[55] S. Logothetidis, M. Cardona, P. Lautenschlager, and M. Garriga, Phys. Rev. B **34**, 2458 (1986).
[56] J. P. Laurenti, J. Camassel, A. Bouhemadou, B. Toulouse, R. Legros, and A. Lusson, J. Appl. Phys. **67**, 6454 (1990).
[57] M. Cardona, Phys. Status Solidi A **188**, 1209 (2001).
[58] R. Pässler, J. Appl. Phys. **90**, 3956 (2001).
[59] J. Hartung, L. Å. Hansson, and J. Weber, Proceedings of the 20th International Conference on the Physics of Semiconductors, Thessaloniki, Greece, edited by E. M. Anastassakis and J. D. Joannopoulos (World Scientific, Singapore, 1990), p. 1875.
[60] V. Alex, S. Finkbeiner, and J. Weber, J. Appl. Phys. **79**, 6943 (1996).
[61] R. Pässler, to be published.
[62] A. V. Mudryi, V. M. Trukhan, A. I. Patuk, I. A. Shakin, and S. F. Marenkin, Fiz. Tekh. Poluprovodn. (S.-Peterburg) **31**, 1029 (1997).
[63] L. W. Tu, Y. C. Lee, K. H. Lee, C. M. Lai, I. Lo, K. Y. Hsieh, and M. Hong, Appl. Phys. Lett. **75**, 2038 (1999).
[64] A. A. Homs and B. Marí, J. Appl. Phys. **88**, 4654 (2000).